Three Decades of Artisanal Gold Mining Reveal Contrasting Outcomes for Conservation Areas and Indigenous Lands

Elmontaserbellah Ammar[1], Sean J. Glynn[1], Kerry Anne Kansinally[2], William Clemens[3], Emilius Richter[3], Matthias Werner[4,5,6], Matthew J. Struebig[1], Jake E. Bicknell[1]

[1] Durrell Institute for Conservation and Ecology (DICE), School of Natural Sciences, University of Kent, Canterbury, UK
[2] Conservation International Guyana, Georgetown, Guyana
[3] dida Datenschmiede GmbH, Berlin, 10827, Germany
[4] Qilimanjaro Quantum Tech, Barcelona, Spain
[5] Universitat de Barcelona Departament de Física Quàntica i Astrofísica, Barcelona, Spain
[6] Universitat de Barcelona Institut de Ciències del Cosmos, ICCUB, Barcelona, Spain

Authors for correspondence: ea588@kent.ac.uk (E.A.); J.E.Bicknell@kent.ac.uk (J.E.B.)

Abstract

Artisanal gold mining (AGM) is a critical driver of tropical forest disturbance, yet is challenging to quantify. Using deep learning and three decades of satellite imagery (1995-2024), we mapped AGM expansion across three contrasting countries in northern Amazonia. We evaluate mining trends, and extent across differing land designations and associated impacts on carbon stocks. AGM area increased >2000% over the study period, evolving from dispersed sites, into larger, consolidated mining landscapes, cumulatively releasing ~27,000 Gg of aboveground carbon from the region. Crucially, we show that protected areas slowed new mine establishment, while Indigenous lands faced rapid, sustained mining intensification, particularly since 2010. These findings show how long-term, high-resolution monitoring and machine learning can support policy responses across governance contexts, including providing key data needed in regulating legal and illegal mining, identifying emerging frontiers, and prioritising areas for restoration or protection where mining pressures intersect biodiversity and carbon priorities.

1. Introduction

Artisanal gold mining (AGM) has emerged as one of the most pervasive drivers of tropical forest disturbance and loss. While agriculture remains the dominant cause of deforestation globally, gold mining is an increasingly important driver in forest-rich regions, particularly across South America (Harlow et al., 2019). At the pantropical scale, industrial mining alone accounted for over 3,000 km^2 of forest loss between 2000 and 2019; meanwhile artisanal operations have driven substantial, but often poorly documented, disturbance across tropical forests (Alvarez-Berríos & Mitchell Aide, 2015; Giljum et al., 2022).

Unlike industrial operations, AGM operates through thousands of small, mobile, and often informal sites, and impacts can be difficult to detect, monitor, and govern using conventional land-use assessments (Adler Miserendino et al., 2013). Despite their relatively small individual footprints, these activities generate persistent surface disturbance, altered hydrology, and long-lasting ecological legacies (Barbarossa et al., 2026; Dethier et al., 2023; Kalamandeen et al., 2020).

The three Guyanas of northeastern Amazonia, spanning Guyana, Suriname, and French Guiana, represent a critical but understudied frontier. The region contains some of the World's most intact tropical forests, characterised by high carbon stocks and biodiversity, as well as protected and Indigenous lands (Groombridge & Jenkins, 2002; Malhi et al., 2006; Roy et al., 2001). Simultaneously, long-standing gold-bearing geological formations have attracted widespread mining, which by 2014 had already disturbed an estimated 160,000 ha of forest across the Guyanas (Rahm et al., 2021). Because large portions of the region's forests remain contiguous, mining expansion here offers an opportunity to examine how dispersed extractive pressures accumulate and intersect with conservation designations before landscapes become heavily transformed - as seen on Indonesia's Bangka-Belitung islands, where artisanal tin mining expanded to half the land area (Jong, 2024; Nurtjahya et al., 2017).

Previous studies have documented AGM-driven deforestation in the Guyanas, yet none have investigated long-term spatiotemporal dynamics, or quantified mining across differing land designations (Alvarez-Berríos & Mitchell Aide, 2015; Dezécache et al., 2017; Rahm et al., 2021). Moreover, most prior research has relied on global mining datasets that provide valuable context, but remain too coarse to reliably detect AGM for detailed analyses (Liang et al., 2021; Maus et al., 2022; Sepin et al., 2025; Tang & Werner, 2023).

Advances in remote sensing and deep learning (Nava et al., 2022; Ronneberger et al., 2015), offer new opportunities to determine whether AGM expansion is episodic or structurally persistent. Using these high-resolution tools, we can interrogate critical questions: Do protected areas, Key Biodiversity Areas (KBAs), and Indigenous lands experience distinct long-term mining trajectories?; Does formal land designation meaningfully constrain mining activity, or merely redistribute it across the landscape?

Here, we reconstruct three decades (1995-2024) of AGM expansion across the Guyanas using a deep-learning-based semantic segmentation approach applied to Landsat imagery. We quantify long-term trends in mining extent, site frequency, and site size; estimate associated aboveground carbon losses; and evaluate how mining trajectories differ across protected areas, KBAs, Indigenous lands, and non-designated forests. By linking spatiotemporal mining dynamics with land governance, this study provides a comprehensive assessment of how AGM reshapes tropical landscapes and identifies where conservation and governance interventions are most likely to face the greatest challenges or hold the most promise.

2. Methods

2.1. Study Region and Period

Our appraisal focuses on the forests of the three countries within the Guiana Shield of the northeastern Amazon basin (Figure 1). To define the study area, we screened Landsat World Reference System (WRS-2) tiles covering Guyana, Suriname, and French Guiana. We retained tiles where AGM was visually detectable in recent (2024) imagery (Figure S1), based on characteristic spectral and spatial features such as excavation pits and tailings. Because abandoned mining sites typically leave persistent surface scars detectable for decades, tiles without visible mining in 2024 were assumed unlikely to contain historical AGM activity (see Figure S2). Our analysis spans 1995-2024, supporting both regional mapping of mining disturbance and spatiotemporal quantification of mining trends within protected areas, KBAs, and Indigenous lands.

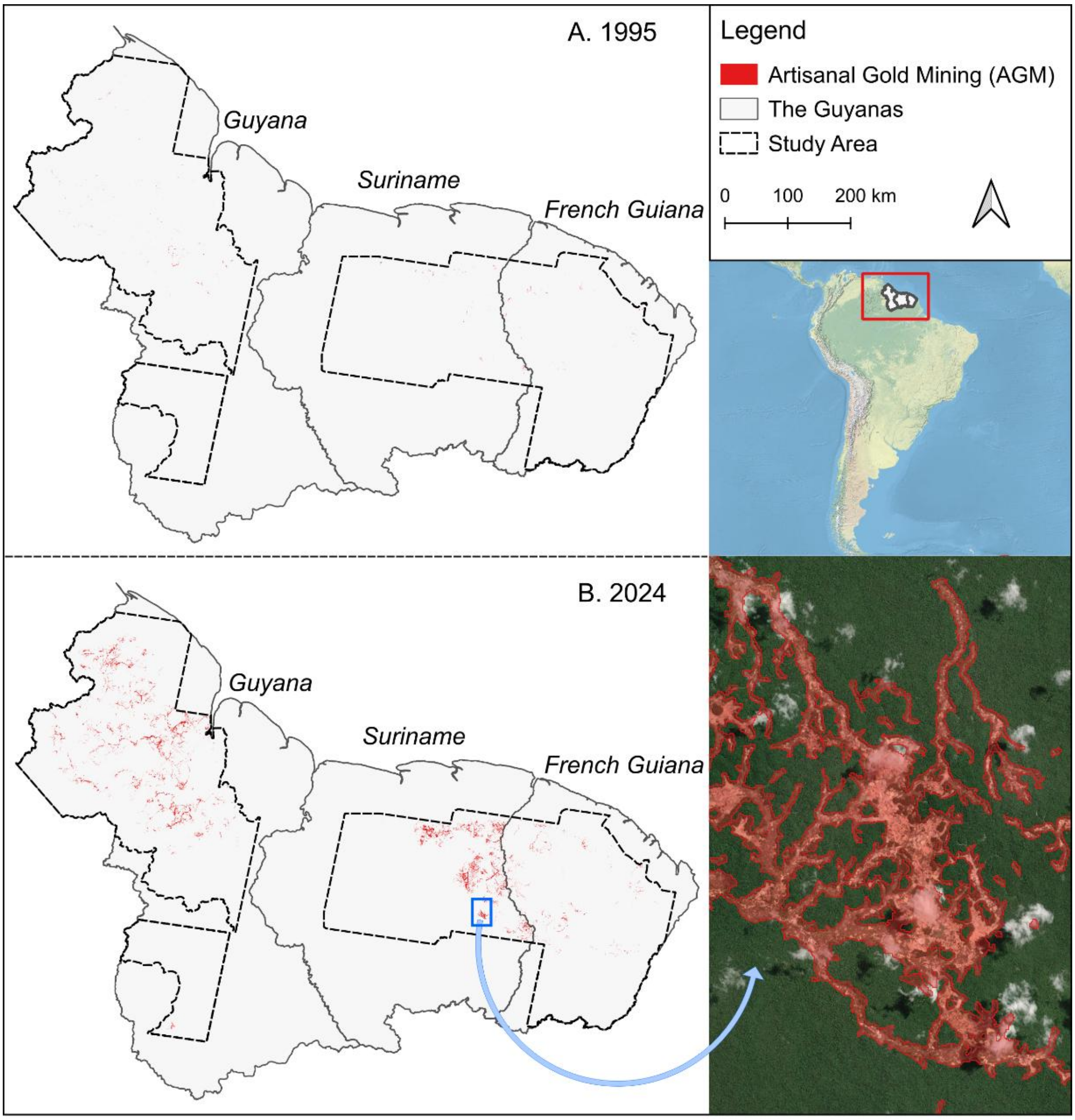

Figure 1: Study area and expansion of artisanal gold mining (AGM) across the Guyanas. Predicted AGM polygons for 1995 (A) and 2024 (B) show the growth and intensification of mining disturbance.

2.2. Mining Disturbance Classification

We mapped AGM using historical Landsat surface reflectance imagery (1995-2024), from Landsat 5 TM, Landsat 8 OLI, and Landsat 9 OLI (Collection 2, Tier-1). Mining was detected using a deep learning semantic segmentation model trained to identify characteristic surface features, including pits, tailings, and exposed soil.

We employed a U-Net-based convolutional neural network (ASMSpotter) (GmbH, 2025; Ronneberger et al., 2015), trained using manual labels of AGM activity from visual interpretation and very high-resolution reference imagery (see Text S1 for technical description of model training, data augmentation, evaluation metrics, and inference post-processing). The model achieved an F1 score of 0.86 (precision = 0.85; recall = 0.86; Figures S3A-E). To minimise cloud-related omission, predictions from all available scenes within each year were combined, and annual mining footprints were vectorised as contiguous polygons for subsequent analysis (Figure S4).

To improve temporal consistency and reduce spurious detections of mining activity, we applied a post-classification filtering step, thereby improving the reliability of our final dataset beyond the 0.86 F1 score produced by the model. This involved filtering out false positives by generating centroids for all annual mining polygons, with kernel density estimation around to identify persistent clusters of mining activity across years. Where the model identified isolated (isolated in time and space) predicted mines, we were then able to conduct a final manual screening step to remove systematic false positives. This occurred primarily in savannah and peatland landscapes that can occasionally exhibit mining-like spectral signatures in Landsat imagery.

2.3. Area Metrics and Trend Summaries

For each year, mine polygon areas were summarised to derive three core metrics: (i) total mapped mining area (sum of polygon areas), (ii) number of mining polygons, and (iii) mean polygon area. These metrics were calculated for the entire study area, by country, and within protected areas, Key Biodiversity Areas (KBAs), and titled Indigenous lands (Supplementary Tables S7-S10).

2.4. Aboveground Carbon Loss Estimation

We estimated aboveground carbon (AGC) loss attributable to mining for 2000-2024 using spatially explicit aboveground biomass data (from Harris et al., 2021). Annual mining area was multiplied by biome-specific aboveground biomass values and converted to carbon using a factor of 0.47 (Goslee et al., 2016). Uncertainty was quantified using lower and upper quartile estimates (see Text S2 for technical description AGC loss calculations).

2.5. Spatiotemporal Overlap with Land Designations

To quantify how AGM intersects with key land designations, the area (ha) of AGM polygons intersecting: protected areas, Key Biodiversity Areas, and Indigenous lands was calculated using the 'Overlap Analysis' tool in QGIS and expressed both as absolute area and as a percentage of total AGM extent.

To quantify the temporal trends of AGM occurrence within land designations, annual mining polygons (1995-2024) were spatially intersected with each designation layer (Protected Areas, Key Biodiversity Areas, and Indigenous Lands) for every year in the study period. We also evaluated AGM occurring outside all designated areas.

To enable fair comparisons across designations of varying size, we calculated mining density per land designation, as mining area per 100 hectares of each land designation, and number of mining polygons per 100 hectares of each land designation. Mean polygon area was retained as an absolute measure.

Results were summarised by land designation type within each country and also aggregated across the Guyanas. Trends were visualised using LOESS smoothing with 95% confidence intervals to reveal temporal trends. Designation boundaries remain fixed throughout the study period. Protected area boundaries were obtained from the World Database on Protected Areas (WDPA) (UNEP-WCMC & IUCN, 2025), KBA boundaries from the global KBA dataset (BirdLife International, 2025), and Indigenous land boundaries for Guyana and French Guiana from the LandMark platform (LandMark: The Global Platform of Indigenous and Community, 2025). These designations are not mutually exclusive, and spatial overlaps occur among protected areas, KBAs, and Indigenous lands. For Suriname, where no officially recognised Indigenous land spatial data are publicly available, Indigenous and Maroon living area boundaries were adapted from Heemskerk (2009) and manually digitised.

3. Results

3.1. Spatiotemporal trajectories of AGM in the Guyanas

Across the Guyanas, cumulative mining area increased 2,097% (from 7,960 ha in 1995 to 174,881 ha in 2024; Figures 1A-B). This expansion was accompanied by a ~900% increase in the number of mining polygons and a steady rise in mean mine size (Figure S5A-C; Table S1). Mining expansion was non-linear, accelerating between 2005 and 2015 before continuing at a moderated rate after 2015 (Figure S5; Table S1).

3.2. National-level trends

In Guyana, the largest country in the study, mining expanded steadily to 96,425 ha by 2024, representing the region's largest absolute footprint. Suriname experienced the most rapid relative expansion, with sharp increases in both total mining extent and mean polygon size. In contrast, French Guiana showed slower and more variable growth, with smaller mean polygon sizes and a comparatively limited total footprint (Figure 2; Tables S2-4). AGM represented 0.45% of Guyana’s land area, 0.46% of Suriname’s, and 0.13% of French Guiana’s (Figure 3B), with higher proportional impacts when restricted to forested areas (Figure 3C; Table S5A).

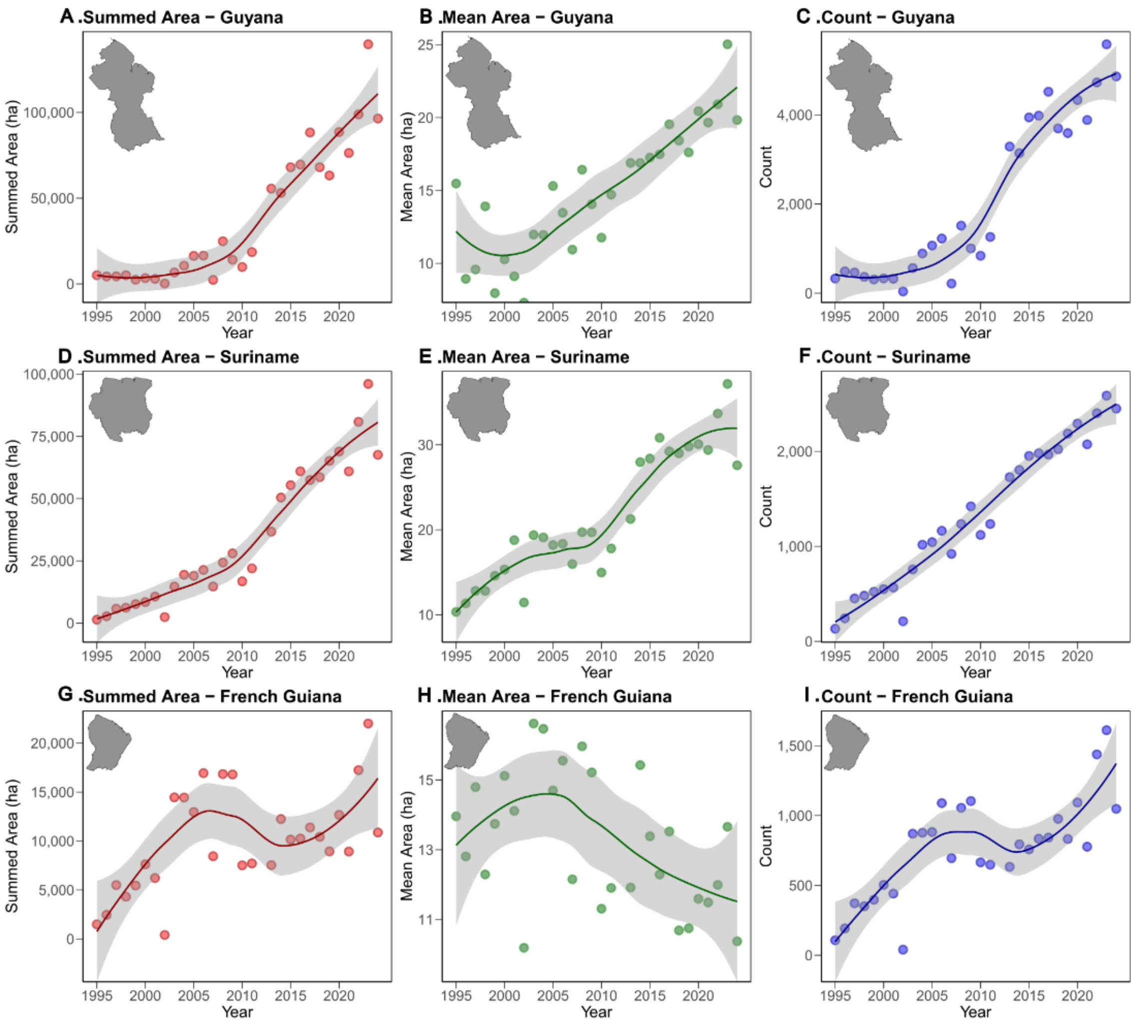

Figure 2: National mining trajectories in Guyana (A-C), Suriname (D-F), and French Guiana (G-I), showing annual mined area, polygon count, and mean polygon size (1995-2024). Lines show loess trends with 95% confidence intervals.

3.3. Aboveground Carbon Loss

Mining-related aboveground carbon loss accumulated substantially between 2000 and 2024 (Figure 3A; Table S6). Total estimated losses were highest in Guyana (median 13,687 Gg C), followed by Suriname (11,785 Gg C), and lowest in French Guiana (1,906 Gg C).

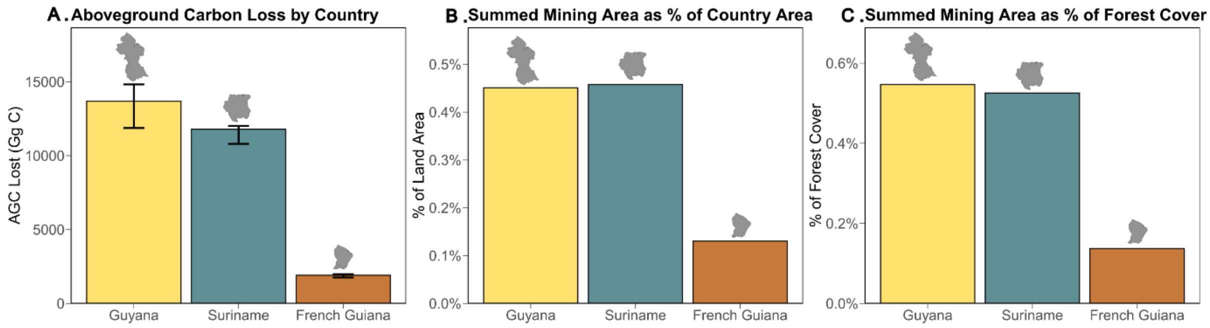

Figure 3: (A) Estimated aboveground carbon (AGC) loss from mining, 2000-2024, with median national losses and uncertainty ranges. (B) Mining area as a percentage of national land area. (C) Mining area as a percentage of national forest cover.

3.4. Mining Extent Across Indigenous Lands, Protected Areas, and KBAs

AGM overlapped with protected areas and Key Biodiversity Areas in all three countries. Notably, in French Guiana, 26.6% of mapped AGM area intersected protected areas, while in Suriname 8.0% overlapped KBAs (Figure 4A-B; Tables S5B-C). AGM activity further intersected Indigenous lands also faced significant encroachment, with overlap reaching 20.3% in Suriname and 9.8% in Guyana, while French Guiana showed lower but non-negligible overlap (4.2%) (Figure 4C; Tables S5B-C).

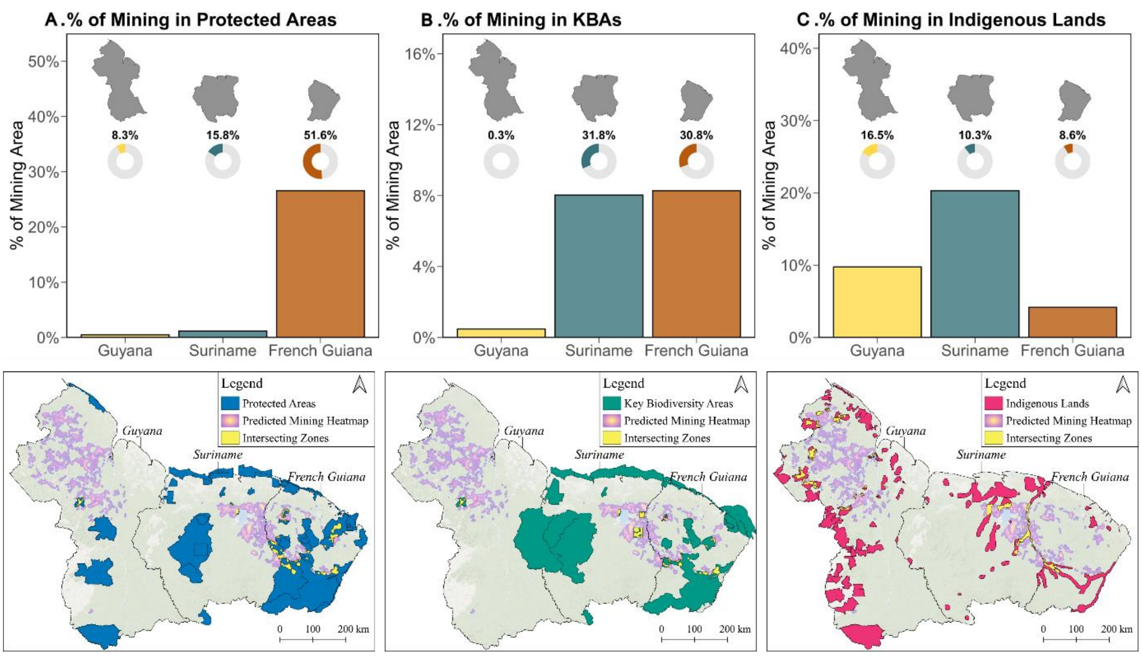

Figure 4: Overlap between mining and land designations: protected areas (A), Key Biodiversity Areas (B), and Indigenous lands (C) in 2024. Bars show the share of national AGM within each designation; donut charts show each designation's share of national land area. Maps show AGM density overlain on each designation. **Suriname's Indigenous boundaries digitised from Heemskerk (2009) due to lack of freely available official spatial data.*

AGM within Indigenous lands increased >1,900%, with total area rising from 1,160 ha in 1995 to 23,988 ha in 2024 (Table S7; Figure 5A-E). This was accompanied by a ~1,900% increase in mine count and a near doubling of mean mine size (10.95-19.50 ha). Intensity accelerated after 2010, with a 350% increase in area between 2010 and 2024.

Within protected areas, AGM rose from 235 ha (1995) to a peak of 5,232 ha in 2008 (2,126% increase) before stabilising and declining through the 2010s (Table S8; Figure 5A-E). By 2024, protected-area AGM had rebounded slightly to 4,217 ha (~1,694% increase of 1995 levels), but remained below the late-2000s peak. Mean mine size increased modestly over most of the time series, then decreased in recent years.

AGM within KBAs increased 8,601%, from 79 ha in 1995 to 6,874 ha in 2024 (Table S9; Figure 5A-E). Post-2010 growth was primarily driven by expansion in mine size (mean polygon area grew from 8.6 ha in 2010 to ~22 ha by 2024), while mine counts stabilised, briefly declined, and then increased again in the late 2010s. Density-normalised KBA intensity increased from 0.11 to 4.26 polygons per 100 ha and from 0.001 to 0.094 ha per 100 ha between 1995 and 2024.

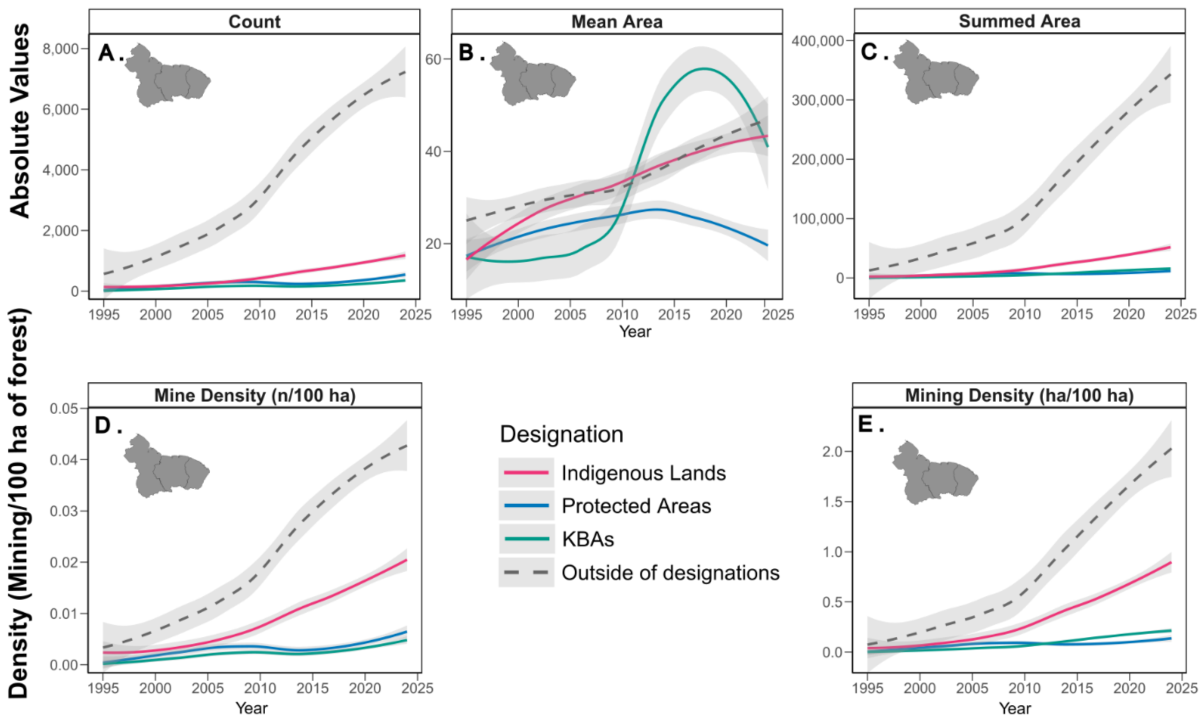

Figure 5: Spatiotemporal (1995-2024) trends of predicted mining polygon sites (≥1 ha) across designation types (Protected Areas: blue, KBAs: teal, Indigenous Lands: pink, and non-designated areas: grey, dashed) in the combined Guyanas. Upper panel shows absolute values (count: A, mean area: B, and summed area: C) of predicted mining polygon sites (≥1 ha) for Protected Areas (blue), KBAs (teal), Indigenous Lands (pink), and non-designated areas (gray, dashed) across Guyana, French Guiana, and Suriname. Lower panel shows density metrics per 100 ha of forest within each designation type (D, E). Lines represent loess-smoothed trends (span = 0.75) with 95% confidence intervals (shaded regions).

National patterns broadly mirrored these regional trajectories but varied in magnitude (Figure 6A-O). Indigenous-land AGM expansion was strongest in Suriname (394-13,912 ha; 3,431% increase; Table S10), followed by Guyana (1,150% increase; Table S11), while French Guiana remained low overall but increased >400% increase after 2018 (Table S12). Within protected areas, French Guiana accounted for the majority of regional AGM, whereas activity in Guyana and Suriname protected areas remained limited and episodic (Tables S13-S15). Suriname dominated regional mining within KBAs, while French Guiana showed lower but persistent activity with a ~500% increase since 2018, largely driven by a rising number of individual mines (Tables S16-S18).

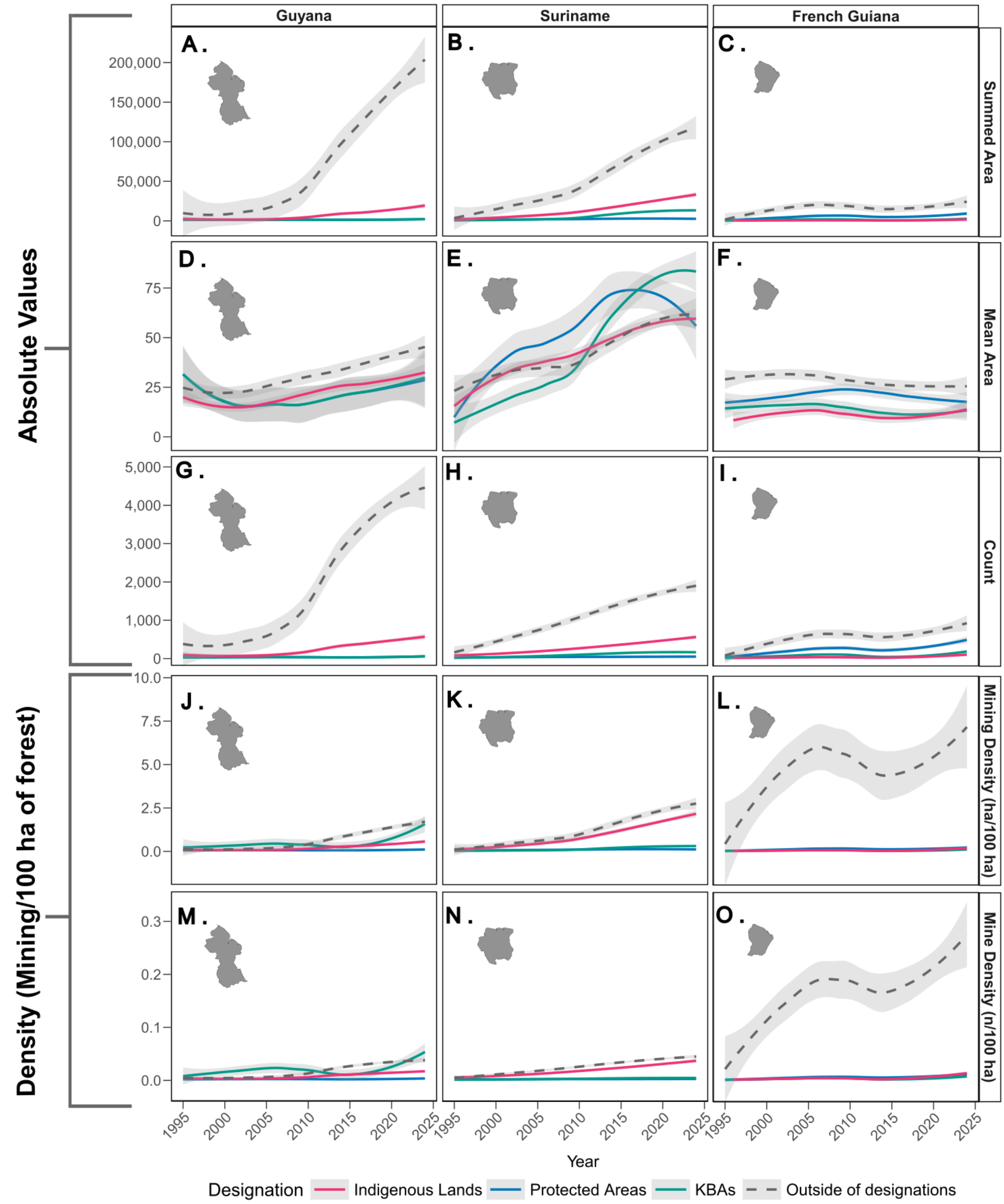

Figure 6: Spatiotemporal (1995-2024) trends of predicted mining polygon sites (≥1 ha) across designation types (Protected Areas: blue, KBAs: teal, Indigenous Lands: pink, and non-designated areas: grey, dashed) in the Guyanas, split up by country. Top grid: Absolute metrics showing total mining area (ha) (A-C), mean mining site size (ha) (D-F), and mine count (G-I). Bottom grid: density metrics showing mining intensity per 100 ha of forest area for summed area (J-L), and

mine density (n/100 ha forest) (M-O). Lines represent loess-smoothed trends (span = 0.75) with 95% confidence intervals (shaded regions).

Trends outside PAs, KBAs, and Indigenous lands broadly mirrored overall trajectories at both regional and national scales, with a strong increase in mining extent and count to a peak in the early 2020s, followed by a slight decline in 2024 (Figures 5-6; Tables S19-S22). For clarity, Figures S6-S7 (regional and national-scale, respectively) show the equivalent trends with areas outside PAs, KBAs, and Indigenous lands omitted.

4. Discussion

Artisanal gold mining (AGM) expanded ~2000% across the Guyanas between 1995 and 2024. Although the rate of AGM expansion slowed after the mid-2010s, this reflects consolidation rather than retreat, with activity increasingly concentrated in larger, contiguous mine-forest landscapes. This pattern mirrors trajectories reported elsewhere in the Amazon and the tropics more broadly, where dispersed exploratory mining sites evolve into larger mining landscapes with long legacies (Asner et al., 2013; Caballero Espejo et al., 2018; Kalamandeen et al., 2020). Increasing mean mine size indicates rising intensity, likely amplifying impacts on forest structure, hydrology, and carbon storage (Barbarossa et al., 2026; Dethier et al., 2023; Sonter et al., 2017).

Our finding that mining rates stabilised and declined within protected areas after the late 2000s suggests that protected designations can constrain the establishment of new AGM sites. Yet mapped mining footprints remained far above 1995 baselines, highlighting the lasting imprint of earlier disturbance within protected area landscapes. Temporary increases in mean mine size further suggest that reductions in mine numbers were not always accompanied by equivalent declines in total disturbed area.

Notably, Indigenous lands experienced a rapid and sustained increase in AGM across the study period, accelerating after 2010, and coinciding with the slowed rate seen in protected areas. These trends were most pronounced in Guyana and

Suriname, where Indigenous lands now host a substantial share of regional AGM activity. Indigenous lands are known globally to be among the most ecologically intact landscapes (Garnett et al., 2018), but here, in the Guyanas region, we show that they are emerging as a primary frontier of AGM expansion. This pattern may reflect the decision of local people to generate income from mining on their land, but it may also represent cases where local communities are unable to prevent unwanted mining. Addressing the latter may require strengthened Indigenous land rights, support for Indigenous-led conservation where sought (e.g., ICCAs), and capacity for increased and coordinated enforcement of unwanted or illegal activities (Sajeva et al., 2019). Unwanted AGM may be concerning for local people on multiple grounds, as it is frequently associated with negative social, cultural, and health impacts, including mercury contamination, in-migration, and loss of subsistence resources (Alamgir et al., 2017; Araruna et al., 2025).

Mining inside KBAs increased sharply after 2010, driven primarily by growth in mine size rather than mine number. This implies that the important biodiversity in KBAs is increasingly threatened by mining in this region. However, a comparison with the global KBA database indicates that mining is rarely listed as a threat for KBAs in the Guyanas, with only one site in French Guiana and none in Suriname or Guyana reporting mining-related pressures (Key Biodiversity Areas Partnership, 2026). This highlights a mismatch between observed mining expansion and recorded threat assessments, which may reflect time lags, incomplete assessments, or differences in how threats are documented. Since KBAs are delineated based on biodiversity value, and only a minority of KBAs are protected (Yang et al., 2025), they may be particularly vulnerable to such habitat degradation, highlighting a gap between this biodiversity prioritisation method and protection.

The estimated loss of ~27,000 Gg of aboveground carbon since 2000 underscores the climate relevance of AGM in the Guyanas. Although modest at continental scales, losses are still substantial. Previous climate modelling has predicted that rapid and sustained forest loss in the Guyanas could destabilise atmospheric processes that distribute moisture across the Amazon basin, with substantial climatic symptoms across the continent (Bovolo et al., 2018), and additional implications for REDD+ and forest-carbon initiatives (Salzman et al., 2018).

Collectively, these findings indicate that conservation strategies centred solely on expanding state-led protected areas are unlikely to curb long-term AGM expansion. Although protected areas appeared to constrain the establishment of new mining sites, most mining activity remained concentrated outside protected-area networks, highlighting the importance of integrating mining dynamics into broader land-use planning and conservation decision-making.

In our study, three decades of mapping reveal artisanal gold mining in the Guyanas as a persistent and consolidating land-use whose impacts are unevenly distributed. Protected areas appear to be capable of slowing the establishment of new mining sites but, so majority of mining continues to occur in forests outside of protection, while among formal land designations, pressure is highest within Indigenous lands and other priority landscapes that underpin regional biodiversity conservation and carbon storage. Our study also suggests that mining impacts are likely to intensify across this region, with current rates steady or increasing. Therefore, governments, conservation practitioners, climate modellers and wider society should expect sustained forest impacts and associated knock-on effects. However, given that mining landscapes are often abandoned after minerals are extracted, these landscapes could provide prospects for forest recovery if left alone or actively restored, but the ever-increasing value and demand for gold may still threaten such opportunities.

Data Accessibility

Mining footprint polygons and associated summary datasets will be made publicly available upon publication via an online repository.

Conflicts of Interest Statement

The authors declare no conflicts of interest.

Author Contributions Statement

Elmontaserbellah Ammar led the conceptualisation, methodology, formal analysis, visualisation, and writing of the manuscript. Emilius Richter, William Clemens, and Matthias Werner contributed to software, model development, and editing. Sean J. Glynn and Kerry Anne Kansinally provided regional expertise and editing. Matthew J. Struebig and Jake E. Bicknell contributed conceptual and methodological guidance, as well as writing. All authors reviewed and edited the manuscript.

Acknowledgements

We thank colleagues at the Durrell Institute for Conservation and Ecology (DICE) for valuable discussion and feedback throughout this project. We are grateful to partners at Dida Datenschmiede GmbH for technical collaboration on model development. We also thank Conservation International Guyana for insights into regional mining dynamics. E.A. was supported by a PhD scholarship from the University of Kent. M.J.S was supported by Research England's 'Expanding Excellence in England' fund.

References

Adler Miserendino, R., Bergquist, B. A., Adler, S. E., Guimarães, J. R. D., Lees, P. S. J., Niquen, W., Velasquez-López, P. C., & Veiga, M. M. (2013). Challenges to measuring, monitoring, and addressing the cumulative impacts of artisanal and small-scale gold mining in Ecuador. *Resources Policy*, *38*(4), 713–722. https://doi.org/10.1016/j.resourpol.2013.03.007

Alamgir, M., Campbell, M. J., Sloan, S., Goosem, M., Clements, G. R., Mahmoud, M. I., & Laurance, W. F. (2017). Economic, Socio-Political and Environmental Risks of Road Development in the Tropics. *Current Biology*, *27*(20), R1130–R1140. https://doi.org/10.1016/j.cub.2017.08.067

Alvarez-Berríos, N. L., & Mitchell Aide, T. (2015). Global demand for gold is another threat for tropical forests. *Environmental Research Letters*, *10*(1), 014006. https://doi.org/10.1088/1748-9326/10/1/014006

Araruna, L. T., de Oliveira, A. T., de Oliveira Novaes, E., de Pinho, J. V., de Almeida Rodrigues, P., & Conte-Junior, C. A. (2025). Mercury contamination endangers Indigenous Amazonian communities: A systematic review. *Environmental Science and Pollution Research*, *32*(23), 13607–13625. https://doi.org/10.1007/s11356-025-36529-7

Asner, G. P., Llactayo, W., Tupayachi, R., & Luna, E. R. (2013). Elevated rates of gold mining in the Amazon revealed through high-resolution monitoring. *Proceedings of the National Academy of Sciences*, *110*(46), 18454–18459. https://doi.org/10.1073/pnas.1318271110

Barbarossa, V., Schipper, A. M., Andringa, I., van Oorschot, M., Sonter, L. J., & Marques, A. (2026). The Many Pathways of Mining Impacts on Biodiversity. *Conservation Letters*, *19*(1), e70000. https://doi.org/10.1111/con4.70000

BirdLife International. (2025). *World Database of Key Biodiversity Areas* [Dataset]. KBA Partnership.

Bovolo, C. I., Wagner, T., Parkin, G., Hein-Griggs, D., Pereira, R., & Jones, R. (2018). The Guiana Shield rainforests—Overlooked guardians of South American climate. *Environmental Research Letters*, *13*(7), 074029. https://doi.org/10.1088/1748-9326/aacf60

Caballero Espejo, J., Messinger, M., Román-Dañobeytia, F., Ascorra, C., Fernandez, L. E., & Silman, M. (2018). Deforestation and Forest Degradation Due to Gold Mining in the Peruvian Amazon: A 34-Year Perspective. *Remote Sensing*, *10*(12), 1903. https://doi.org/10.3390/rs10121903

Dethier, E. N., Silman, M., Leiva, J. D., Alqahtani, S., Fernandez, L. E., Pauca, P., Çamalan, S., Tomhave, P., Magilligan, F. J., Renshaw, C. E., & Lutz, D. A. (2023). A global rise in alluvial mining increases sediment load in tropical rivers. *Nature*, *620*(7975), 787–793. https://doi.org/10.1038/s41586-023-06309-9

Dezécache, C., Faure, E., Gond, V., Salles, J.-M., Vieilledent, G., & Hérault, B. (2017). Gold-rush in a forested El Dorado: Deforestation leakages and the need for regional cooperation. *Environmental Research Letters*, *12*(3), 034013. https://doi.org/10.1088/1748-9326/aa6082

Giljum, S., Maus, V., Kuschnig, N., Luckeneder, S., Tost, M., Sonter, L. J., & Bebbington, A. J. (2022). A pantropical assessment of deforestation caused by industrial mining. *Proceedings of the National Academy of Sciences*, *119*(38), e2118273119. https://doi.org/10.1073/pnas.2118273119

GmbH, dida D. (2025). *ASMSpotter Demo: Detecting Artisanal Mining Activity Using AI*. https://dida.do/demos/asmspotter

Goslee, K., Walker, S. M., Grais, A., Murray, L., Casarim, F., & Brown, S. (2016). Module C-CS: calculations for estimating carbon stocks. *LEAF Technical*

Guidance Series for the Development of a Forest Carbon Monitoring System for REDD.

Groombridge, B., & Jenkins, M. (2002). *World atlas of biodiversity: Earth's living resources in the 21st century*. Univ of California Press.

Harlow, D., Hurley, K., Fox, A., Vargas-Guerra, A., & Gibson, J. (2019). Small-scale & artisanal mining: Impacts on biodiversity in Latin America. *Washington, DC: The Cadmus Group and USAID*.

Harris, N. L., Gibbs, D. A., Baccini, A., Birdsey, R. A., de Bruin, S., Farina, M., Fatoyinbo, L., Hansen, M. C., Herold, M., Houghton, R. A., Potapov, P. V., Suarez, D. R., Roman-Cuesta, R. M., Saatchi, S. S., Slay, C. M., Turubanova, S. A., & Tyukavina, A. (2021). Global maps of twenty-first century forest carbon fluxes. *Nature Climate Change*, *11*(3), 234–240. https://doi.org/10.1038/s41558-020-00976-6

Jong, H. N. (2024). A tarnished reputation: Corruption at the heart of Indonesia's state-owned tin mining sector that is wrecking the environment. *Global Initiative Against Transnational Organized Crime*. https://globalinitiative.net/

Kalamandeen, M., Gloor, E., Johnson, I., Agard, S., Katow, M., Vanbrooke, A., Ashley, D., Batterman, S. A., Ziv, G., Holder-Collins, K., & others. (2020). Limited biomass recovery from gold mining in Amazonian forests. *Journal of Applied Ecology*, *57*(9), 1730–1740.

Key Biodiversity Areas Partnership. (2026). *Key Biodiversity Areas factsheet: Atachi Bakka*. https://www.keybiodiversityareas.org/site/factsheet/23899/assessment

LandMark: The Global Platform of Indigenous and Community, L. (2025). *Indigenous Peoples' Lands and Territories and Local Community Lands* [Dataset]. LandMark Global Platform.

Liang, T., Werner, T. T., Heping, X., Jingsong, Y., & Zeming, S. (2021). A global-scale spatial assessment and geodatabase of mine areas. *Global and Planetary Change*, *204*, 103578. https://doi.org/10.1016/j.gloplacha.2021.103578

Malhi, Y., Wood, D., Baker, T. R., Wright, J., Phillips, O. L., Cochrane, T., Meir, P., Chave, J., Almeida, S., Arroyo, L., Higuchi, N., Killeen, T. J., Laurance, S. G., Laurance, W. F., Lewis, S. L., Monteagudo, A., Neill, D. A., Vargas, P. N., Pitman, N. C. A., … Vinceti, B. (2006). The regional variation of aboveground live biomass in old-growth Amazonian forests. *Global Change Biology*, *12*(7), 1107–1138. https://doi.org/10.1111/j.1365-2486.2006.01120.x

Maus, V., Giljum, S., da Silva, D. M., Gutschlhofer, J., da Rosa, R. P., Luckeneder, S., Gass, S. L. B., Lieber, M., & McCallum, I. (2022). An update on global mining land use. *Scientific Data*, *9*(1), 433. https://doi.org/10.1038/s41597-022-01547-4

Nava, L., Cuevas, M., Meena, S., Catani, F., & Monserrat, O. (2022). Artisanal and Small-Scale Mine Detection in Semi-Desertic Areas by Improved U-

Net. *IEEE GEOSCIENCE AND REMOTE SENSING LETTERS*, *19*. (WOS:000891200500005). https://doi.org/10.1109/LGRS.2022.3220487

Nurtjahya, E., Franklin, J. A., Fournita Agustina, S., & others. (2017). The Impact of tin mining in Bangka Belitung and its reclamation studies. *Sriwijaya International Conference on Engineering, Science and Technology (SICEST 2016)*, *101*(6).

Rahm, M., Smartt, T., Paloeng, C., Kasanpawiro, C., Moe Soe Let, V., Pichot, C., Bedeau, C., Farias, P., Carvalho, R., & Villien, C. (2021). Monitoring the impact of gold mining on the forest cover and freshwater in the Guiana Shield. *Reference Year*, *60*, pp40.

Ronneberger, O., Fischer, P., & Brox, T. (2015). *U-Net: Convolutional Networks for Biomedical Image Segmentation* (arXiv:1505.04597). arXiv. https://doi.org/10.48550/arXiv.1505.04597

Roy, J., Saugier, B., & Mooney, H. A. (2001). *Terrestrial global productivity*. Academic Press.

Sepin, P., Vashold, L., & Kuschnig, N. (2025). Mapping mining areas in the tropics from 2016 to 2024. *Nature Sustainability*, *8*(11), 1400–1407. https://doi.org/10.1038/s41893-025-01668-9

Sonter, L. J., Herrera, D., Barrett, D. J., Galford, G. L., Moran, C. J., & Soares-Filho, B. S. (2017). Mining drives extensive deforestation in the Brazilian Amazon. *Nature Communications*, *8*(1), 1013. https://doi.org/10.1038/s41467-017-00557-w

Tang, L., & Werner, T. T. (2023). Global mining footprint mapped from high-resolution satellite imagery. *Communications Earth & Environment*, *4*(1), 134. https://doi.org/10.1038/s43247-023-00805-6

Yang, R., Dong, X., Xu, S., Li, X., Wang, K., Ye, Y., & Xiao, W. (2025). Unveiling human impacts on global Key Biodiversity Areas: Assessing disturbance and fragmentation to inform conservation strategies. *Geography and Sustainability*, *6*(3), 100259. https://doi.org/10.1016/j.geosus.2024.100259

UNEP-WCMC and IUCN (2025) Protected Planet: The World Database on Protected Areas (WDPA), 06/2025, Cambridge, UK: UNEP-WCMC and IUCN. Available at: www.protectedplanet.net.

Supplementary Materials

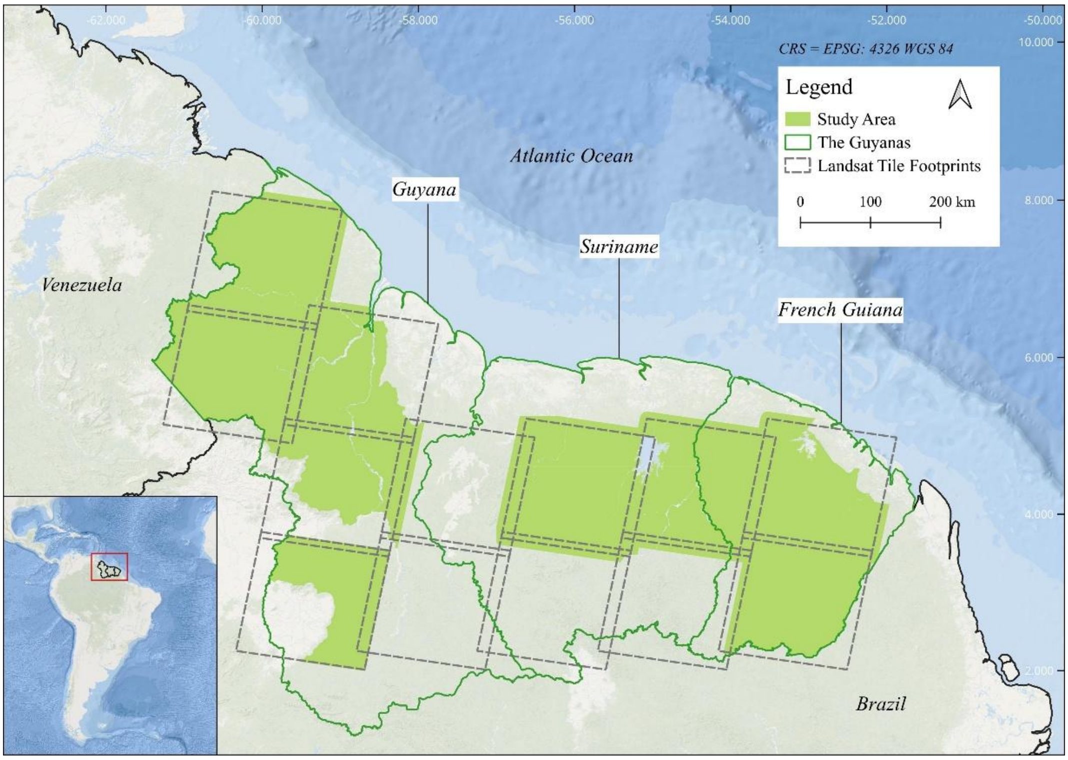

Figure S1: Landsat tiles inspected, and the final study area spanning parts of Guyana, Suriname, and French Guiana within the Guyanas.

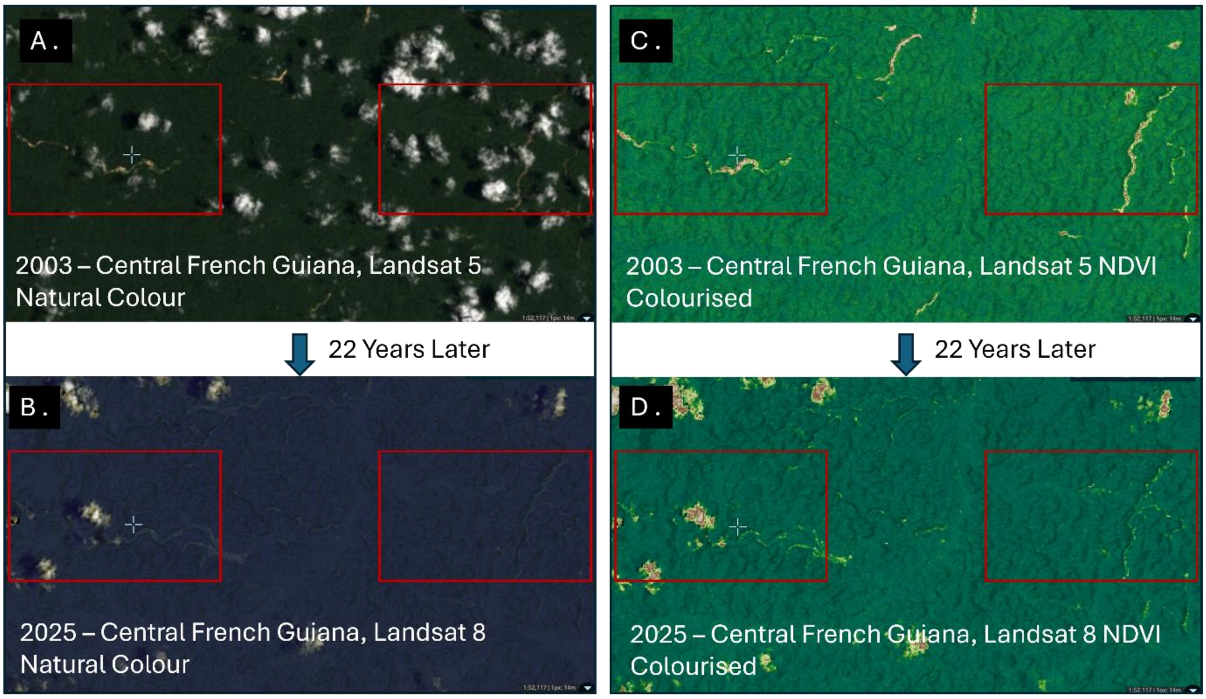

Figure S2: Persistence of artisanal gold mining surface scars in Landsat imagery. The same site in central French Guiana shown in 2003 (Landsat 5) and 2025

(Landsat 8) in natural colour (A-B) and NDVI (C-D), illustrating long-term detectability of abandoned mining disturbance.

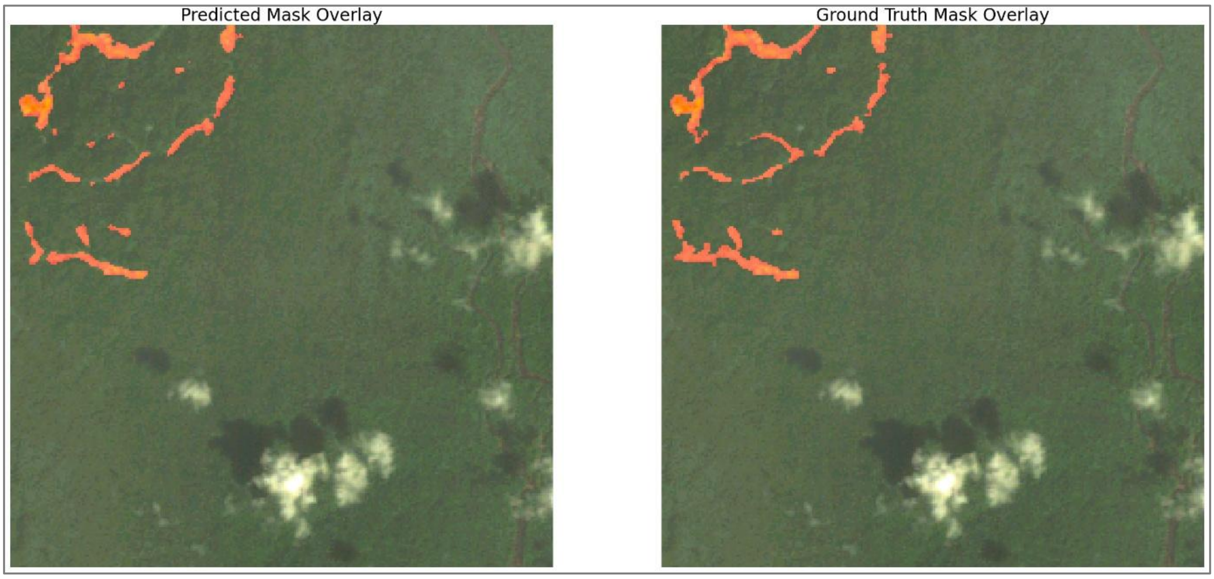

Figure S3A: Example from the independent test dataset showing model predictions compared with manually digitised reference labels. The panel displays one of thirty held-out Landsat tiles (256 × 256 pixels; 30 m resolution) containing a mixture of artisanal gold mining (AGM) and non-mining areas, illustrating model performance on previously unseen imagery.

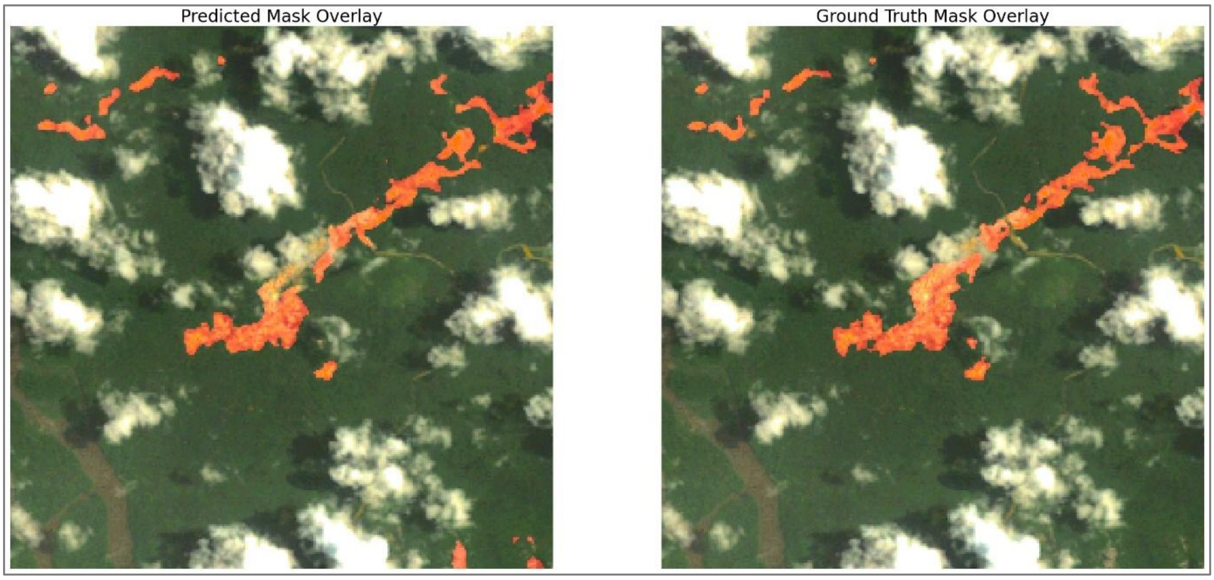

Figure S3B: Example from the independent test dataset showing model predictions compared with manually digitised reference labels. The panel displays one of thirty held-out Landsat tiles (256 × 256 pixels; 30 m resolution) containing a mixture of artisanal gold mining (AGM) and non-mining areas, illustrating model performance on previously unseen imagery.

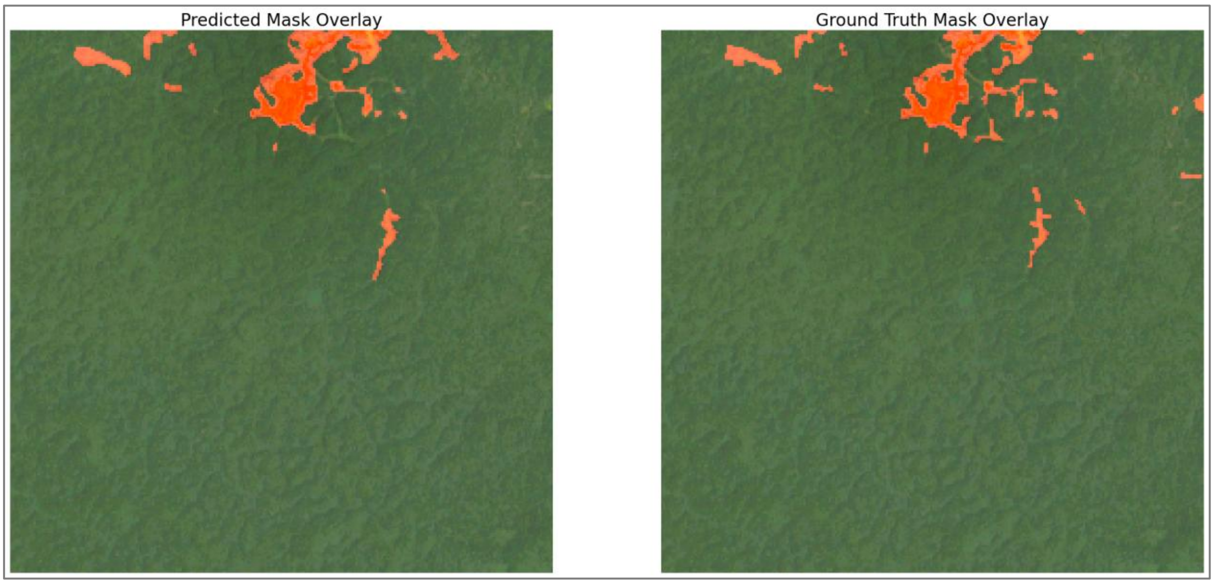

Figure S3C: Example from the independent test dataset showing model predictions compared with manually digitised reference labels. The panel displays one of thirty held-out Landsat tiles (256 × 256 pixels; 30 m resolution) containing a mixture of artisanal gold mining (AGM) and non-mining areas, illustrating model performance on previously unseen imagery.

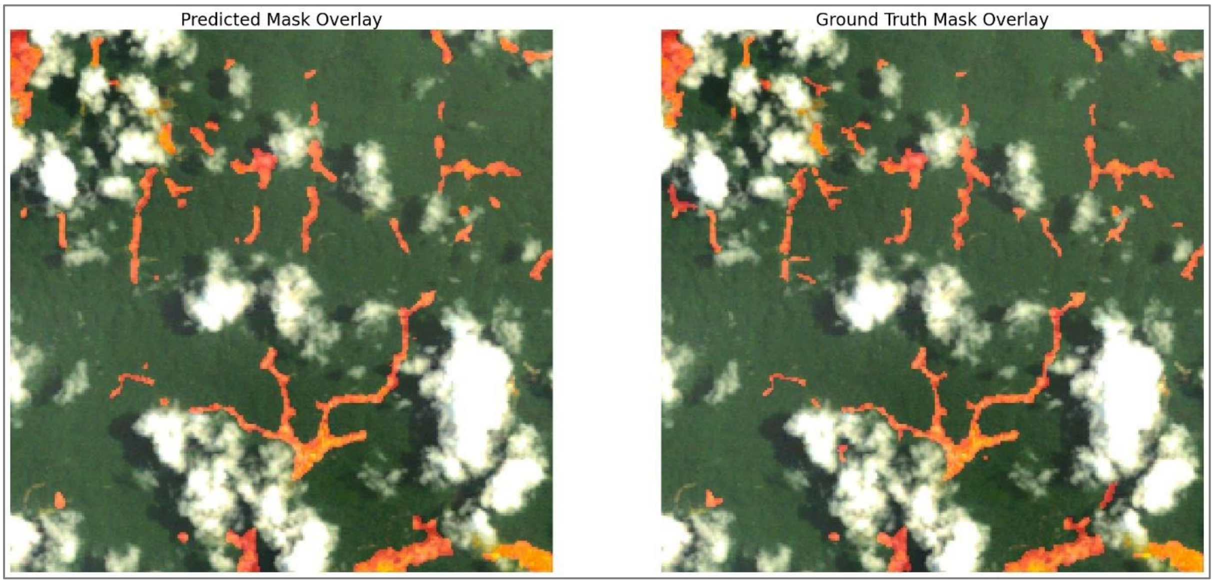

Figure S3D: Example from the independent test dataset showing model predictions compared with manually digitised reference labels. The panel displays one of thirty held-out Landsat tiles (256 × 256 pixels; 30 m resolution) containing a mixture of artisanal gold mining (AGM) and non-mining areas, illustrating model performance on previously unseen imagery.

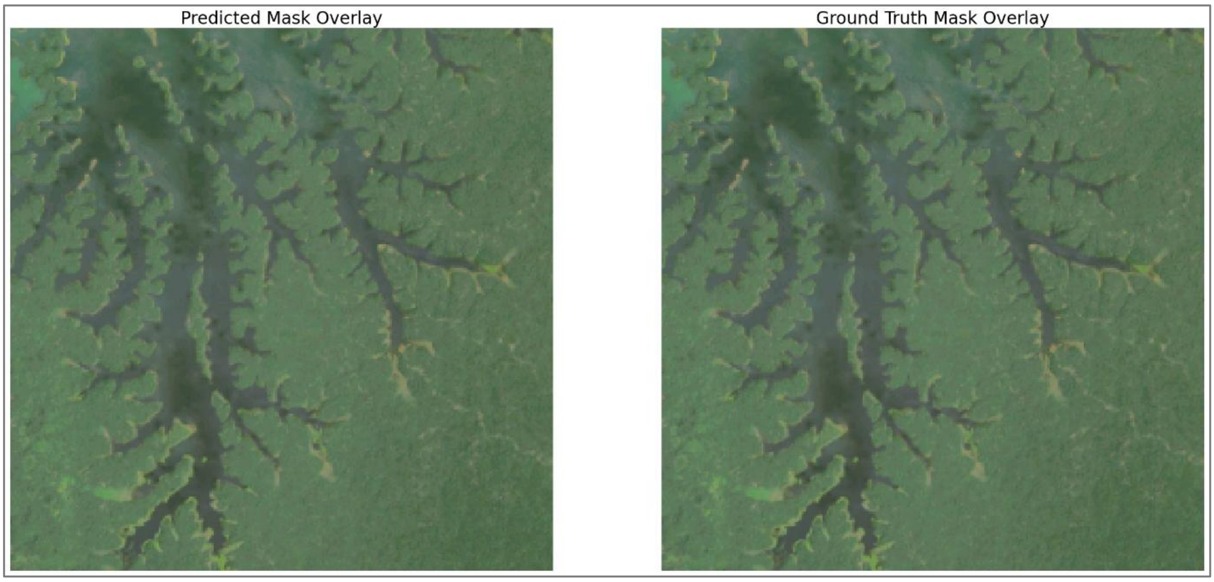

Figure S3E: Example from the independent test dataset showing model predictions compared with manually digitised reference labels. The panel displays one of thirty held-out Landsat tiles (256 × 256 pixels; 30 m resolution) containing a mixture of artisanal gold mining (AGM) and non-mining areas, illustrating model performance on previously unseen imagery.

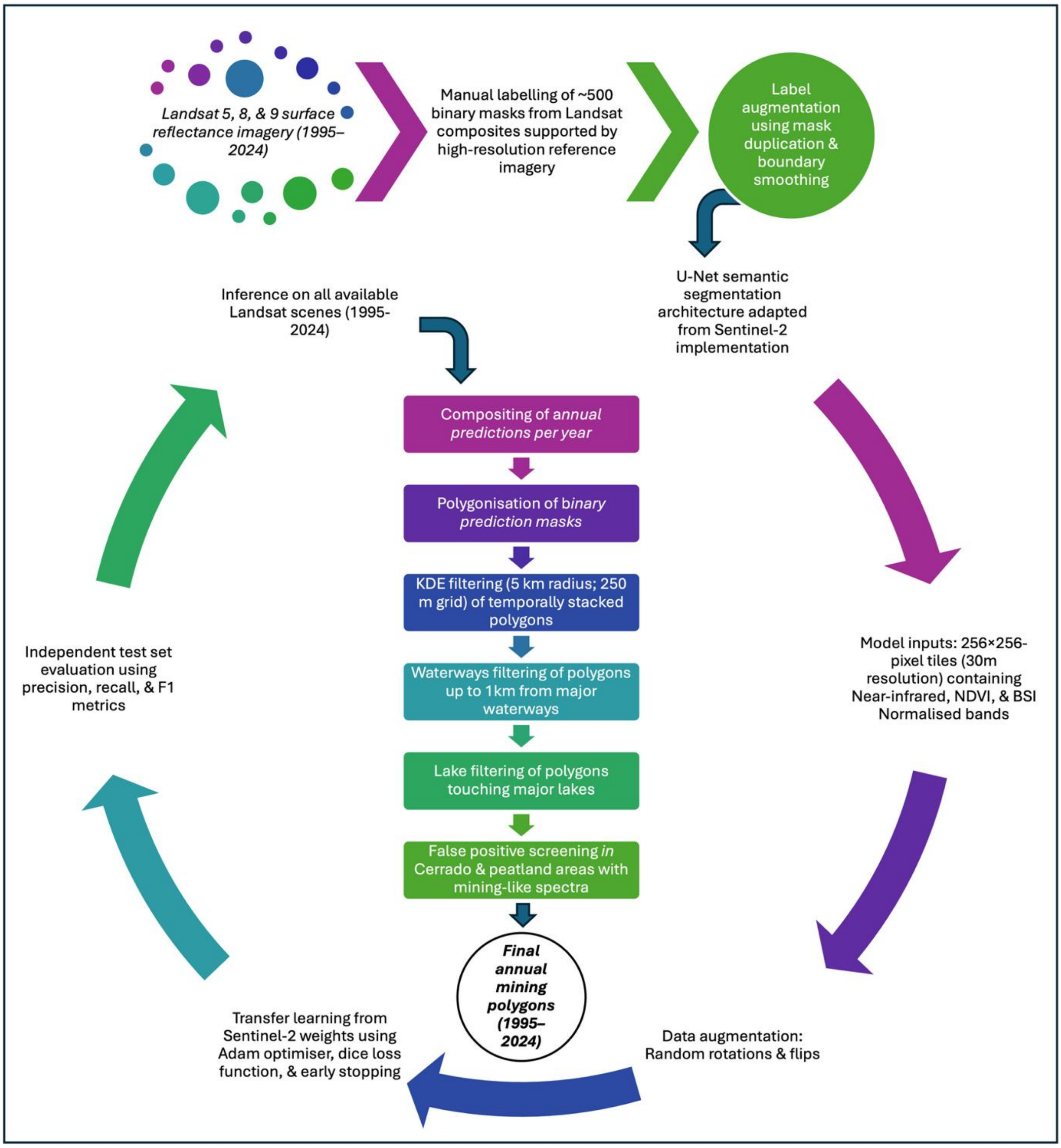

Figure S4: Flow diagram showing the workflow of model training, inference, and post-processing of outputs.

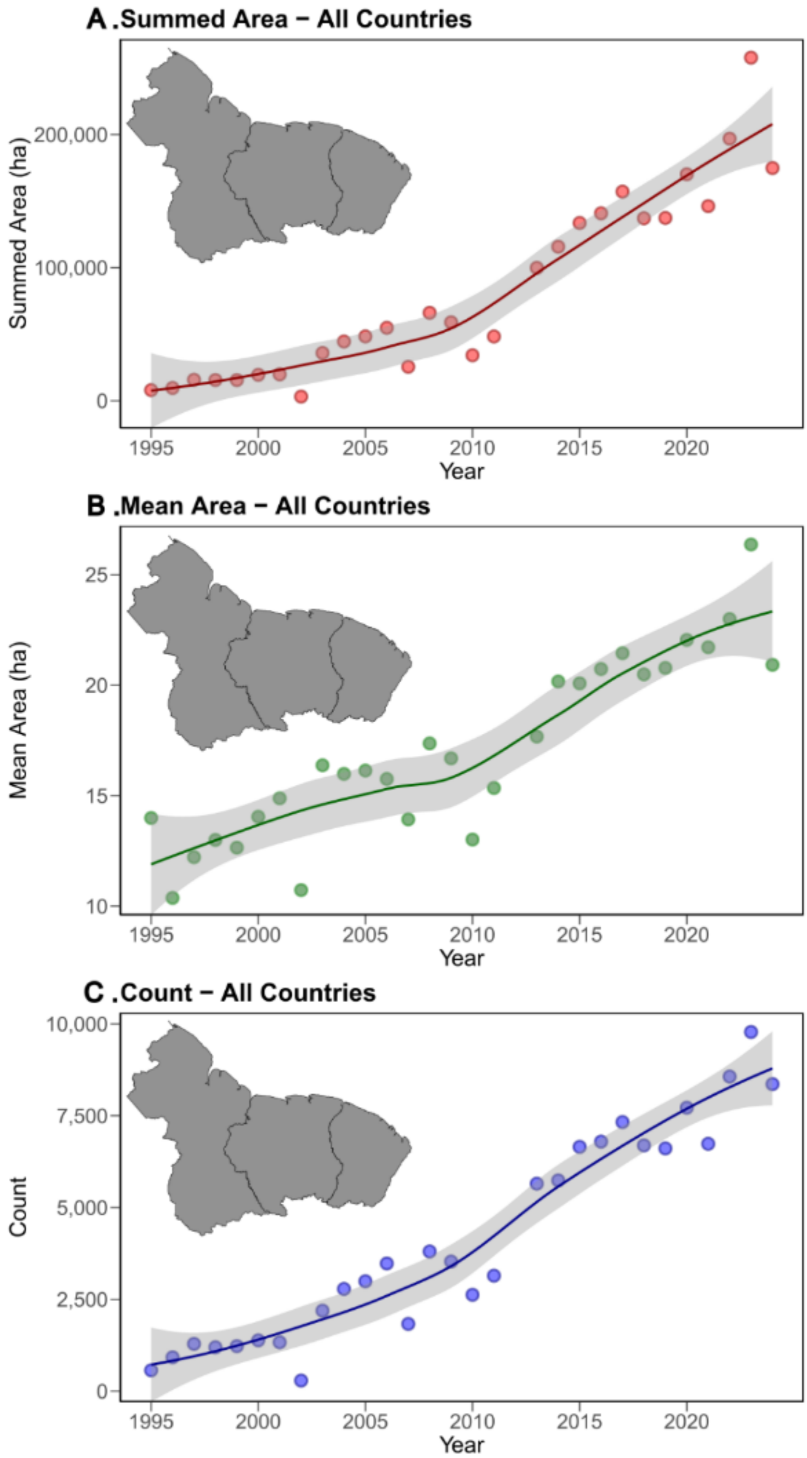

Figure S5: Temporal trajectories of AGM across the Guyanas (1995-2024). (A) Total mapped mining area (ha) per year. (B) Number of mining polygons per year. (C) Mean mining polygon size (ha) per year. Lines show loess trends with 95% confidence intervals.

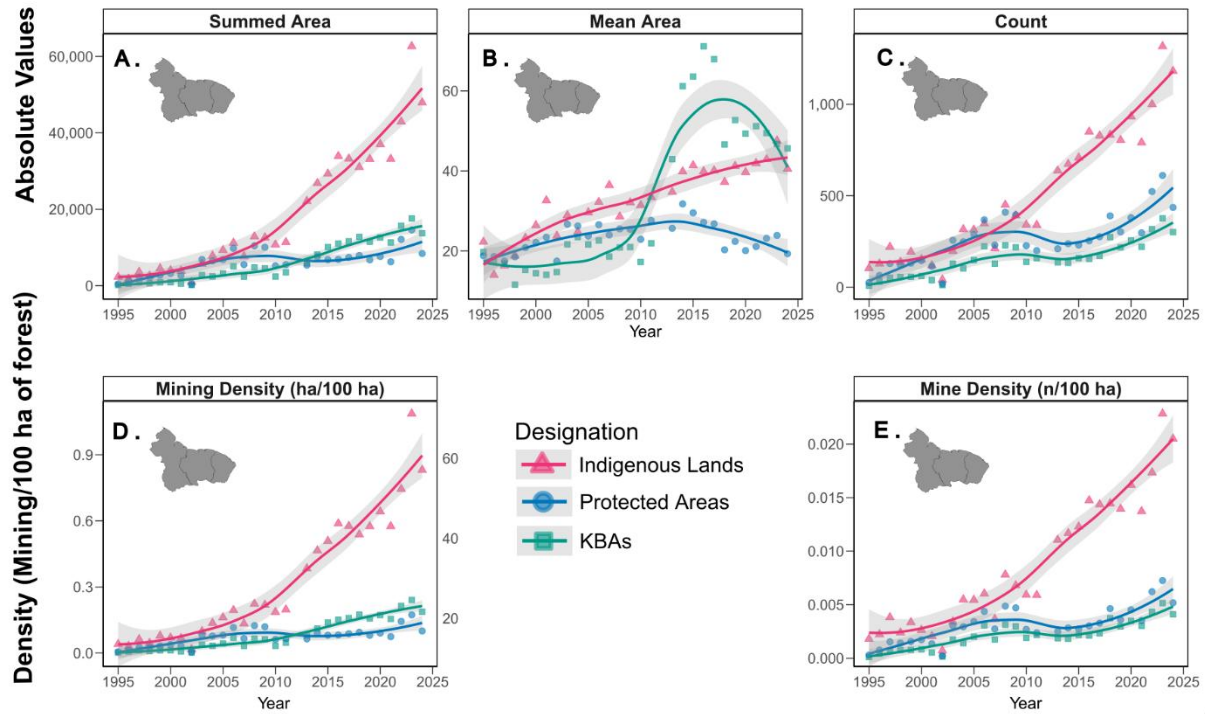

Figure S6: Spatiotemporal trends (1995-2024) in predicted mining polygons (≥1 ha) across protected areas, KBAs, and Indigenous lands in the combined Guyanas. Upper panels show absolute trends (area, mean size, count); lower panels show mining density per 100 ha of forest in that land use designation. Loess trends include 95% confidence intervals.

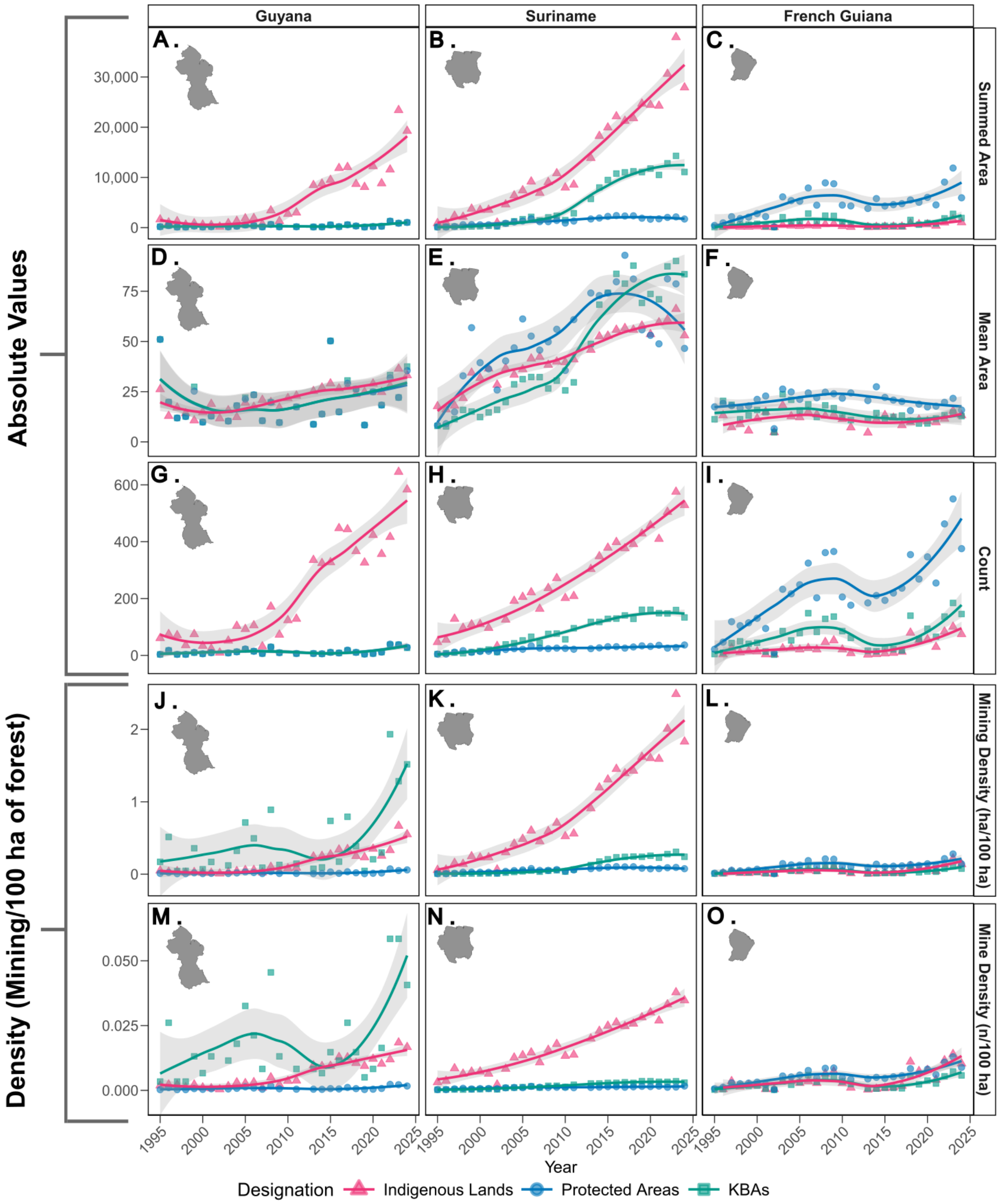

Figure S7: National level spatiotemporal trends (1995-2024) in predicted mining polygons (≥1 ha) across protected areas, KBAs, and Indigenous lands. Top panels (A-I) show absolute metrics (area, mean size, count); bottom panels (J-O) show density normalised metrics per 100 ha of forest. Loess trends include 95% confidence intervals.

Text S1: Deep Learning Training and Inference Workflow

Purpose

Manual interpretation of ~700 Landsat scenes across three decades is not feasible. We therefore developed an automated deep-learning workflow to detect artisanal gold mining activity consistently across space and time.

Model architecture

ASMSpotter is a U-Net–based convolutional neural network designed for semantic segmentation of heterogeneous mining features in satellite imagery (Ronneberger et al., 2015). The model was adapted from an existing Sentinel-2 implementation and retrained for Landsat imagery.

Training data and labelling

We created ~500 manually delineated binary training masks from Landsat composites and very high-resolution reference imagery (e.g. Google Earth). Masks captured a range of mining typologies (active, abandoned, clustered, dispersed) across tropical forest landscapes. To increase label diversity and improve generalisation, each mask was duplicated and redrawn using smoother boundary styles, producing ~1,000 training samples.

Data augmentation

Training samples were randomly rotated and flipped to reduce orientation bias and overfitting. Each training tile consisted of a 256 × 256-pixel Landsat patch (30 m resolution) composed of near-infrared reflectance, NDVI, and Bare Soil Index layers. All inputs were normalised prior to training.

Training procedure

The model was initialised using pre-trained Sentinel-2 weights and retrained using the Landsat-labelled dataset. Optimisation employed the Adam algorithm with a Dice loss objective function to balance mining and non-mining class representation. Training used 788 tiles for training and 196 for validation. Early stopping was applied once validation loss stabilised.

Model evaluation

Performance was assessed using an independent test set and evaluated using precision, recall, and *F*1 metrics:

$$Precision = \frac{True\ Positives}{True\ Positives + False\ Positives}$$

$$Recall = \frac{True\ Positives}{True\ Positives + False\ Negatives}$$

$$F1 = 2 \times \frac{Precision \times Recall}{Precision + Recall}$$

The final model achieved *F*1 = 0.855, precision = 0.849, and recall = 0.861.

Inference and post-processing

All Landsat surface reflectance scenes were processed through the trained model using PyTorch. Raster handling employed Rasterio, and binary prediction masks were vectorised into polygon shapefiles. To minimise cloud-related omission, predictions from all available scenes within each year were merged to produce annual mining footprints. Figure S4 illustrates the inference and post-processing workflow.

Text S2: Aboveground Carbon Loss Estimation

To quantify potential carbon losses driven by AGM, Aboveground Biomass (AGB) statistics were derived from the 2000 aboveground biomass dataset provided by Harris et al. (2021). Since this dataset reflects biomass values as of the year 2000, we constrained our Aboveground Carbon (AGC) loss estimates to the period 2000–2024. Although our dataset included mining activity from 1995 onward, we could not quantify the associated biomass loss prior to 2000 due to the lack of AGB baseline data for earlier years. As such, AGC loss values represent post-2000 forest carbon loss attributable to gold mining.

To estimate AGC loss from forests due to AGM activity, we applied a biomass-to-carbon conversion approach based on our annual predicted mining extents described above. For the year 2024, we multiplied the total mined area (in hectares) by the median AGB per hectare for the rainforest biome of the Guyanas. The resulting biomass value was then multiplied by a conversion factor of 0.47 (reflecting the proportion of biomass that is carbon) (Goslee et al., 2016) and converted from megagrams (Mg) to gigagrams (Gg) by dividing by 1000. The general formula used to calculate the midpoint estimate (AGC loss median) is:

$$AGC_{loss}(Gg) = Area_{mined} \times AGB_{per\ ha}(Mg/ha) \times \left(\frac{0.47}{1000}\right)$$

Where: $AGC_{loss}(Gg)$ is the aboveground carbon lost in gigagrams, $Area_{mined}$ is the annual sum of predicted AGM area in hectares, $AGB_{per\ ha}(Mg/ha)$ is the median aboveground biomass in megagrams per hectare, 0.47 is the standard biomass-to-carbon conversion factor for tropical forests, and 1000 is used to convert the final carbon estimate from megagrams to gigagrams.

To provide an estimate of uncertainty in AGC loss, we repeated this calculation using the lower quartile (Q1) and upper quartile (Q3) values of AGB per hectare, also derived from the same source. This yielded two additional AGC loss estimates: $AGC_{loss}(Gg)\mathrm{min}$ (using Q1 AGB), and $AGC_{loss}(Gg)\mathrm{max}$ (using Q3 AGB).

Table S1: Annual count, annual mean area (ha), and annual sum of area (ha) results for all three countries combined. *Note: 2012 is omitted due to the transition between Landsat 5 TM and Landsat 8 OLI. Landsat 7 ETM+ was excluded because of SLC-off artefacts, resulting in insufficient consistent imagery for that year.*

Year	Count	Mean Area (ha)	Sum of Area (ha)
1995	569	13.99	7960
1996	924	10.37	9585
1997	1289	12.22	15748
1998	1197	13.00	15557
1999	1228	12.65	15532
2000	1385	14.05	19453
2001	1332	14.88	19823

2002	290	10.73	3111
2003	2192	16.37	35892
2004	2784	15.99	44502
2005	2994	16.14	48313
2006	3478	15.76	54795
2007	1832	13.93	25512
2008	3805	17.37	66074
2009	3530	16.69	58915
2010	2625	13.01	34161
2011	3145	15.35	48266
2013	5650	17.67	99848
2014	5739	20.16	115723
2015	6652	20.08	133567
2016	6794	20.73	140821
2017	7327	21.45	157131
2018	6692	20.49	137110
2019	6610	20.78	137336
2020	7718	22.05	170147
2021	6735	21.71	146239
2022	8566	22.99	196937
2023	9779	26.36	257788
2024	8360	20.92	174880

Table S2: Table of annual count, annual mean area (ha), and annual sum of area (ha) results for Guyana. *Note: 2012 is omitted due to the transition between Landsat 5 TM and Landsat 8 OLI. Landsat 7 ETM+ was excluded because of SLC-off artefacts, resulting in insufficient consistent imagery for that year.*

Year	Count	Mean Area (ha)	Sum of Area (ha)
1995	329	15.5	5091
1996	489	8.9	4369
1997	465	9.6	4454
1998	365	13.9	5078
1999	309	8.0	2458
2000	331	10.3	3399
2001	324	9.1	2953
2002	38	7.3	277

2003	564	12.0	6753
2004	890	11.9	10635
2005	1068	15.3	16349
2006	1226	13.5	16513
2007	216	10.9	2364
2008	1515	16.4	24885
2009	1005	14.1	14128
2010	840	11.8	9877
2011	1262	14.7	18567
2013	3289	16.9	55555
2014	3141	16.9	53042
2015	3942	17.3	68028
2016	3981	17.5	69594
2017	4518	19.5	88273
2018	3694	18.4	68066
2019	3591	17.6	63247
2020	4333	20.4	88570
2021	3884	19.7	76365
2022	4727	20.9	98854
2023	5582	25.0	139705
2024	4862	19.8	96425

Table S3: Table of annual count, annual mean area (ha), and annual sum of area (ha) results for Suriname. *Note: 2012 is omitted due to the transition between Landsat 5 TM and Landsat 8 OLI. Landsat 7 ETM+ was excluded because of SLC-off artefacts, resulting in insufficient consistent imagery for that year.*

Year	Count	Mean Area (ha)	Sum of Area (ha)
1995	133	10.34	1375
1996	243	11.35	2757
1997	452	12.81	5790
1998	481	12.82	6164
1999	522	14.59	7617
2000	550	15.33	8433
2001	567	18.78	10647
2002	212	11.45	2426
2003	758	19.37	14680

2004	1017	19.10	19426
2005	1044	18.20	18999
2006	1163	18.35	21345
2007	921	15.96	14702
2008	1235	19.71	24345
2009	1421	19.70	27988
2010	1120	14.97	16763
2011	1235	17.80	21985
2013	1728	21.27	36750
2014	1804	27.96	50432
2015	1952	28.38	55394
2016	1979	30.81	60977
2017	1967	29.22	57471
2018	2022	28.99	58615
2019	2187	29.79	65146
2020	2292	30.06	68906
2021	2074	29.39	60946
2022	2401	33.67	80841
2023	2586	37.15	96080
2024	2450	27.59	67583

Table S4: Annual count, annual mean area (ha), and annual sum of area (ha) results for French Guiana. *Note: 2012 is omitted due to the transition between Landsat 5 TM and Landsat 8 OLI. Landsat 7 ETM+ was excluded because of SLC-off artefacts, resulting in insufficient consistent imagery for that year.*

Year	Count	Mean Area (ha)	Sum of Area (ha)
1995	107	14.00	1493
1996	192	12.80	2459
1997	372	14.80	5503
1998	351	12.30	4314
1999	397	13.70	5455
2000	504	15.10	7619
2001	441	14.10	6223
2002	40	10.20	407
2003	870	16.60	14457
2004	877	16.50	14441

2005	882	14.70	12964
2006	1089	15.60	16936
2007	695	12.20	8445
2008	1055	16.00	16844
2009	1104	15.20	16798
2010	665	11.30	7520
2011	648	11.90	7713
2013	633	11.90	7542
2014	794	15.40	12248
2015	758	13.40	10145
2016	834	12.30	10249
2017	842	13.50	11386
2018	976	10.70	10429
2019	832	10.70	8943
2020	1093	11.60	12671
2021	777	11.50	8926
2022	1438	12.00	17241
2023	1611	13.70	22002
2024	1048	10.40	10872

Table S5A: National land, forest, and mining extent in the year 2024. All areas in ha.

Country	Land area	Forest area	Mining area
Guyana	21,392,577	17,631,800	96,425
French Guiana	8,342,389	7,926,590	10,873
Suriname	14,762,001	12,859,300	67,583

Table S5B: Overlap between mining and land designations. All areas in ha. Percentages indicate proportion of national mining area overlapping each designation. *Abbreviations; Protected Areas - PA, Key Biodiversity Areas - KBA, Indigenous Lands - IL.*

Country	Mining in PA	% of mining	Mining in KBA	% of mining	Mining in IL	% of mining
Guyana	469.6	0.49	460.3	0.48	9,416.4	9.77

French Guiana	2,888.8	26.57	900.1	8.28	453.9	4.18
Suriname	792.2	1.17	5,425.4	8.03	13,723.3	20.31

Table S5C: Total land designated as protected, KBA, and Indigenous. All areas in ha. *Abbreviations; Protected Areas - PA, Key Biodiversity Areas - KBA, Indigenous Lands - IL.*

Country	PA area	PA count	KBA area	KBA count	IL area	IL count
Guyana	1,779,712	6	61,704	1	3,522,113	118
French Guiana	4,304,840	39	2,570,096	16	717,932	22
Suriname	2,332,533	21	4,687,701	13	1,524,666	20

Table S6: Table shows lower quartile AGB p/ha (in the year 2000), median AGB p/ha (in the year 2000), upper quartile AGB p/ha, interquartile range AGB p/ha, and AGC (Gg C) lost (minimum, median, and maximum estimates with a conversion factor of 0.47) by 2024 for each of the three countries in the study area. Median (min-max) - Gg AGC values are rounded up to the nearest whole number.

Country	Q1 AGB	Q2 AGB	Q3 AGB	Median (min-max) - Gg AGC
Guyana	262	302	327	13,687 (11,870 – 14,820)
Suriname	340	371	378	11,785 (10,800 – 12,007)
French Guiana	344	373	387	1,906 (1,758 – 1,978)

Table S7: Annual count, annual mean area (ha), annual sum of area (ha), annual count density (d = count/100 ha), and annual sum of area density (d = sum of area ha/100 ha) results for mining within Indigenous lands across all three countries combined. *Note: 2012 is omitted due to the transition between Landsat 5 TM and Landsat 8 OLI. Landsat 7 ETM+ was excluded because of SLC-off artefacts, resulting in insufficient consistent imagery for that year.*

Year	Count	Mean Area (ha)	Sum of Area (ha)	Count (d)	Sum of Area (d)

1995	106	10.95	1160	0.18	0.02
1996	138	6.54	902	0.24	0.02
1997	227	7.92	1798	0.39	0.03
1998	142	9.16	1300	0.25	0.02
1999	194	11.57	2245	0.34	0.04
2000	155	12.96	2009	0.27	0.04
2001	121	16.07	1944	0.21	0.03
2002	42	11.62	487	0.07	0.01
2003	204	13.98	2851	0.35	0.05
2004	329	11.93	3923	0.57	0.07
2005	325	14.33	4655	0.56	0.08
2006	356	15.76	5609	0.62	0.10
2007	216	17.81	3846	0.38	0.07
2008	462	13.93	6433	0.80	0.11
2009	399	15.79	6298	0.69	0.11
2010	350	15.33	5363	0.61	0.09
2011	347	16.41	5695	0.60	0.10
2013	667	16.61	11081	1.16	0.19
2014	693	19.37	13421	1.20	0.23
2015	736	19.92	14663	1.28	0.25
2016	882	19.24	16964	1.53	0.29
2017	863	19.26	16621	1.50	0.29
2018	866	17.93	15524	1.50	0.27
2019	832	19.94	16585	1.44	0.29
2020	958	19.33	18520	1.66	0.32
2021	825	20.12	16598	1.43	0.29
2022	1030	20.85	21470	1.79	0.37
2023	1364	22.98	31347	2.37	0.54
2024	1230	19.50	23987	2.13	0.42

Table S8: Annual count, annual mean area (ha), annual sum of area (ha), annual count density (d = count/100 ha), and annual sum of area density (d = sum of area ha/100 ha) results for mining within protected areas across all three countries combined. *Note: 2012 is omitted due to the transition between Landsat 5 TM and Landsat 8 OLI. Landsat 7 ETM+ was excluded because of SLC-off artefacts, resulting in insufficient consistent imagery for that year.*

Year	Count	Mean Area (ha)	Sum of Area (ha)	Count (d)	Sum of Area (d)
1995	25	9.40	235	0.3	0.03
1996	65	9.18	596	0.77	0.07
1997	132	8.55	1128	1.57	0.13
1998	122	9.12	1112	1.45	0.13
1999	135	10.14	1368	1.6	0.16
2000	147	10.93	1606	1.75	0.19
2001	117	11.44	1338	1.39	0.16
2002	20	8.32	166	0.24	0.02
2003	261	13.15	3431	3.1	0.41

2004	257	12.68	3259	3.05	0.39
2005	295	11.60	3420	3.5	0.41
2006	375	13.05	4891	4.46	0.58
2007	233	11.85	2760	2.77	0.33
2008	413	12.67	5232	4.91	0.62
2009	407	12.37	5033	4.84	0.6
2010	228	11.41	2602	2.71	0.31
2011	204	13.55	2763	2.42	0.33
2013	214	12.61	2697	2.54	0.32
2014	241	15.69	3781	2.86	0.45
2015	233	14.59	3399	2.77	0.4
2016	261	13.22	3450	3.1	0.41
2017	279	13.25	3695	3.32	0.44
2018	401	9.88	3963	4.77	0.47
2019	310	10.91	3382	3.68	0.4
2020	389	9.82	3818	4.62	0.45
2021	305	10.29	3139	3.62	0.37
2022	537	11.30	6065	6.38	0.72
2023	624	11.71	7305	7.41	0.87
2024	451	9.35	4217	5.36	0.5

Table S9: Annual count, annual mean area (ha), annual sum of area (ha), annual count density (d = count/100 ha), and annual sum of area density (d = sum of area ha/100 ha) results for mining within Key Biodiversity Areas across all three countries combined. *Note: 2012 is omitted due to the transition between Landsat 5 TM and Landsat 8 OLI. Landsat 7 ETM+ was excluded because of SLC-off artefacts, resulting in insufficient consistent imagery for that year.*

Year	Count	Mean Area (ha)	Sum of Area (ha)	Count (d)	Sum of Area (d)
1995	8	9.87	78	0.11	0.001
1996	30	8.67	260	0.41	0.004
1997	54	8.13	439	0.74	0.006
1998	61	5.35	326	0.83	0.004
1999	60	7.27	436	0.82	0.006
2000	63	7.01	441	0.86	0.006
2001	40	6.88	275	0.55	0.004
2002	11	7.37	81	0.15	0.001
2003	131	10.59	1387	1.79	0.019
2004	109	11.12	1211	1.49	0.017
2005	149	10.74	1600	2.04	0.022
2006	231	10.99	2537	3.16	0.035
2007	130	9.16	1191	1.78	0.016
2008	233	10.27	2392	3.18	0.033
2009	225	10.18	2290	3.08	0.031
2010	140	8.58	1200	1.91	0.016
2011	163	10.71	1746	2.23	0.024
2013	139	21.02	2921	1.9	0.04

2014	134	30.37	4069	1.83	0.056
2015	160	31.60	5056	2.19	0.069
2016	157	35.13	5515	2.14	0.075
2017	176	33.01	5809	2.4	0.079
2018	286	22.35	6393	3.91	0.087
2019	228	25.22	5749	3.12	0.079
2020	265	23.82	6313	3.62	0.086
2021	230	24.61	5661	3.14	0.077
2022	329	23.84	7842	4.49	0.107
2023	388	22.72	8815	5.3	0.12
2024	312	22.03	6873	4.26	0.094

Table S10: Annual count, annual mean area (ha), annual sum of area (ha), annual count density (d = count/100 ha), and annual sum of area density (d = sum of area ha/100 ha) results for mining within Indigenous lands in Suriname. *Note: 2012 is omitted due to the transition between Landsat 5 TM and Landsat 8 OLI. Landsat 7 ETM+ was excluded because of SLC-off artefacts, resulting in insufficient consistent imagery for that year.*

Year	Count	Mean Area (ha)	Sum of Area (ha)	Count (d)	Sum of Area (d)
1995	46	8.56	393	3.017	0.026
1996	54	7.84	423	3.541	0.028
1997	129	8.77	1131	8.461	0.074
1998	96	10.66	1023	6.297	0.067
1999	108	16.93	1828	7.083	0.120
2000	109	15.66	1706	7.153	0.112
2001	96	17.96	1724	6.299	0.113
2002	32	13.67	437	2.099	0.029
2003	128	17.63	2256	8.397	0.148
2004	194	16.26	3153	12.728	0.207
2005	209	17.54	3666	13.712	0.241
2006	224	20.27	4539	14.698	0.298
2007	165	20.66	3408	10.827	0.224
2008	241	18.60	4483	15.81	0.294
2009	271	19.78	5359	17.781	0.352
2010	204	19.33	3942	13.383	0.259
2011	212	19.95	4228	13.911	0.277
2013	307	22.43	6885	20.142	0.452
2014	351	25.85	9074	23.026	0.596
2015	384	25.83	9919	25.196	0.651
2016	400	27.58	11030	26.241	0.724
2017	386	27.42	10584	25.322	0.694
2018	399	27.18	10844	26.176	0.712
2019	430	28.60	12296	28.211	0.807
2020	460	26.46	12169	30.176	0.799
2021	416	29.07	12092	27.297	0.794
2022	509	29.98	15261	33.401	1.002

2023	585	32.34	18921	38.383	1.242
2024	538	25.86	13911	35.315	0.913

Table S11: Annual count, annual mean area (ha), annual sum of area (ha), annual count density (d = count/100 ha), and annual sum of area density (d = sum of area ha/100 ha) results for mining within Indigenous lands in Guyana. *Note: 2012 is omitted due to the transition between Landsat 5 TM and Landsat 8 OLI. Landsat 7 ETM+ was excluded because of SLC-off artefacts, resulting in insufficient consistent imagery for that year.*

Year	Count	Mean Area (ha)	Sum of Area (ha)	Count (d)	Sum of Area (d)
1995	60	12.77	766	1.704	0.022
1996	82	5.69	466	2.328	0.013
1997	73	7.97	581	2.074	0.017
1998	36	6.62	238	1.022	0.007
1999	73	5.23	381	2.074	0.011
2000	34	6.89	234	0.966	0.007
2001	23	8.92	205	0.653	0.006
2002	8	5.73	45	0.227	0.001
2003	53	7.33	388	1.506	0.011
2004	109	5.68	619	3.095	0.018
2005	95	9.22	875	2.698	0.025
2006	108	8.28	893	3.067	0.025
2007	30	10.33	309	0.852	0.009
2008	175	9.50	1662	4.970	0.047
2009	76	7.88	598	2.159	0.017
2010	127	10.36	1315	3.607	0.037
2011	129	11.21	1446	3.664	0.041
2013	358	11.71	4193	10.172	0.119
2014	338	12.82	4331	9.602	0.123
2015	346	13.62	4711	9.830	0.134
2016	473	12.46	5892	13.440	0.167
2017	465	12.89	5991	13.209	0.170
2018	389	11.07	4307	11.050	0.122
2019	349	11.48	4007	9.916	0.114
2020	442	13.74	6073	12.556	0.173
2021	379	11.54	4372	10.768	0.124
2022	434	13.24	5745	12.327	0.163
2023	673	17.34	11669	19.121	0.332
2024	618	15.54	9601	17.558	0.273

Table S12: Annual count, annual mean area (ha), annual sum of area (ha), annual count density (d = count/100 ha), and annual sum of area density (d = sum of area ha/100 ha) results for mining within Indigenous lands in French Guiana. *Note: 2012 is omitted due to the transition between Landsat 5 TM and Landsat 8 OLI. Landsat 7 ETM+ was excluded because of SLC-off artefacts, resulting in insufficient consistent imagery for that year. Additionaly, 1995 is ommited due to no data available.*

Year	Count	Mean Area (ha)	Sum of Area (ha)	Count (d)	Sum of Area (d)
1995	No Data	No Data	No Data	No Data	No Data
1996	2	6.49	12	0.28	0.002
1997	25	3.42	85	3.48	0.012
1998	10	3.89	38	1.39	0.005
1999	13	2.69	34	1.81	0.005
2000	12	5.70	68	1.67	0.01
2001	2	7.35	14	0.28	0.002
2002	2	2.27	4	0.28	0.001
2003	23	8.97	206	3.2	0.029
2004	26	5.78	150	3.62	0.021
2005	21	5.43	114	2.92	0.016
2006	24	7.37	176	3.34	0.025
2007	21	6.11	128	2.92	0.018
2008	46	6.25	287	6.4	0.04
2009	52	6.57	341	7.24	0.048
2010	19	5.55	105	2.65	0.015
2011	6	3.47	20	0.84	0.003
2013	2	1.10	2	0.28	0.0003
2014	4	4.04	16	0.56	0.002
2015	6	5.44	32	0.84	0.005
2016	9	4.67	42	1.25	0.006
2017	12	3.70	44	1.67	0.006
2018	78	4.77	372	10.86	0.052
2019	53	5.31	281	7.38	0.039
2020	56	4.96	277	7.8	0.039
2021	30	4.46	133	4.18	0.019
2022	87	5.34	464	12.12	0.065
2023	106	7.14	756	14.76	0.105
2024	74	6.41	473	10.31	0.066

Table S13: Annual count, annual mean area (ha), annual sum of area (ha), annual count density (d = count/100 ha), and annual sum of area density (d = sum of area ha/100 ha) results for mining within protected areas in French Guiana. *Note: 2012 is omitted due to the transition between Landsat 5 TM and Landsat 8 OLI. Landsat 7 ETM+ was excluded because of SLC-off artefacts, resulting in insufficient consistent imagery for that year.*

Year	Count	Mean Area (ha)	Sum of Area (ha)	Count (d)	Sum of Area (d)
1995	20	8.61	172	0.47	0.04
1996	45	9.47	426	1.05	0.10
1997	119	8.77	1043	2.77	0.24
1998	105	8.14	854	2.44	0.20
1999	116	8.63	1000	2.70	0.23
2000	130	10.39	1351	3.02	0.31
2001	94	11.18	1051	2.19	0.24

2002	8	3.17	25	0.19	0.01
2003	234	12.88	3014	5.44	0.70
2004	221	11.98	2647	5.14	0.62
2005	252	10.27	2588	5.86	0.60
2006	329	11.86	3901	7.65	0.91
2007	203	10.79	2189	4.72	0.51
2008	362	12.19	4413	8.41	1.03
2009	373	11.60	4325	8.67	1.01
2010	205	10.71	2195	4.77	0.51
2011	179	11.81	2114	4.16	0.49
2013	184	10.13	1863	4.28	0.43
2014	211	13.49	2845	4.90	0.66
2015	194	10.84	2103	4.51	0.49
2016	224	10.03	2245	5.21	0.52
2017	237	9.86	2337	5.51	0.54
2018	362	7.49	2711	8.42	0.63
2019	271	9.15	2480	6.30	0.58
2020	350	8.47	2963	8.14	0.69
2021	259	8.58	2222	6.02	0.52
2022	472	9.52	4492	10.97	1.04
2023	557	10.57	5888	12.95	1.37
2024	382	7.67	2928	8.88	0.68

Table S14: Annual count, annual mean area (ha), annual sum of area (ha), annual count density (d = count/100 ha), and annual sum of area density (d = sum of area ha/100 ha) results for mining within protected areas in Guyana. *Note: 2012 is omitted due to the transition between Landsat 5 TM and Landsat 8 OLI. Landsat 7 ETM+ was excluded because of SLC-off artefacts, resulting in insufficient consistent imagery for that year. Additionaly, 2002 and 2010 are ommited due to no data available.*

Year	Count	Mean Area (ha)	Sum of Area (ha)	Count (d)	Sum of Area (d)
1995	2	25.41	50	0.112	0.002856
1996	16	9.80	156	0.899	0.008806
1997	2	5.84	11	0.112	0.000656
1998	2	6.20	12	0.112	0.000697
1999	9	12.52	112	0.506	0.006331
2000	5	3.93	19	0.281	0.001104
2001	8	6.31	50	0.449	0.002835
2002	No Data	No Data	No Data	No Data	No Data
2003	7	5.08	35	0.393	0.001997
2004	12	8.21	98	0.674	0.005533
2005	21	10.54	221	1.18	0.012443
2006	14	10.80	151	0.786	0.008494
2007	5	5.16	25	0.281	0.001451
2008	28	9.74	272	1.573	0.015327
2009	9	4.19	37	0.506	0.002119

2010	No Data	No Data	No Data	No Data	No Data
2011	5	8.60	42	0.281	0.002414
2013	6	3.61	21	0.337	0.001217
2014	4	6.82	27	0.225	0.001532
2015	9	25.02	225	0.506	0.012663
2016	7	7.37	51	0.393	0.002899
2017	17	14.46	245	0.956	0.013817
2018	10	11.85	118	0.562	0.006664
2019	4	3.06	12	0.225	0.000688
2020	7	8.91	62	0.393	0.003504
2021	10	9.05	90	0.562	0.005084
2022	38	15.81	600	2.136	0.033766
2023	38	10.40	395	2.136	0.022194
2024	28	17.02	476	1.574	0.026777

Table S15: Annual count, annual mean area (ha), annual sum of area (ha), annual count density (d = count/100 ha), and annual sum of area density (d = sum of area ha/100 ha) results for mining within protected areas in Suriname. *Note: 2012 is omitted due to the transition between Landsat 5 TM and Landsat 8 OLI. Landsat 7 ETM+ was excluded because of SLC-off artefacts, resulting in insufficient consistent imagery for that year.*

Year	Count	Mean Area (ha)	Sum of Area (ha)	Count (d)	Sum of Area (d)
1995	3	4.02	12	0.129	0.000517
1996	4	3.48	13	0.172	0.000597
1997	11	6.68	73	0.471	0.003149
1998	15	16.34	245	0.643	0.010505
1999	10	25.55	255	0.429	0.010952
2000	12	19.60	235	0.514	0.010085
2001	15	15.77	236	0.643	0.010143
2002	12	11.76	141	0.514	0.006048
2003	20	19.08	381	0.857	0.016356
2004	24	21.40	513	1.029	0.022008
2005	22	27.76	610	0.943	0.026174
2006	32	26.22	839	1.371	0.035965
2007	25	21.83	545	1.072	0.023384
2008	23	23.72	545	0.986	0.023378
2009	25	26.81	670	1.072	0.028735
2010	23	17.67	406	0.986	0.017427
2011	20	30.33	606	0.857	0.026007
2013	24	33.87	812	1.029	0.034837
2014	26	34.94	908	1.114	0.038927
2015	30	35.70	1070	1.286	0.045903
2016	30	38.43	1152	1.286	0.049412
2017	25	44.50	1112	1.072	0.04771
2018	29	39.08	1133	1.243	0.048596
2019	35	25.43	890	1.501	0.038164

2020	32	24.78	792	1.372	0.0339778
2021	36	22.96	826	1.543	0.035431
2022	27	36.02	972	1.158	0.041699
2023	29	35.24	1021	1.243	0.043799
2024	41	19.80	811	1.758	0.034802

Table S16: Annual count, annual mean area (ha), annual sum of area (ha), annual count density (d = count/100 ha), and annual sum of area density (d = sum of area ha/100 ha) results for mining within Key Biodiversity Areas in French Guiana. *Note: 2012 is omitted due to the transition between Landsat 5 TM and Landsat 8 OLI. Landsat 7 ETM+ was excluded because of SLC-off artefacts, resulting in insufficient consistent imagery for that year.*

Year	Count	Mean Area (ha)	Sum of Area (ha)	Count (d)	Sum of Area (d)
1995	3	5.52	16	0.117	0.000644
1996	8	10.10	80	0.311	0.003142
1997	44	8.71	383	1.712	0.014912
1998	51	5.20	265	1.984	0.010317
1999	42	6.03	253	1.635	0.009846
2000	44	7.66	337	1.712	0.013117
2001	12	7.23	86	0.467	0.003373
2002	1	2.27	2	0.039	0.000088
2003	86	11.49	988	3.346	0.038464
2004	52	10.17	528	2.023	0.020589
2005	77	7.67	590	2.996	0.022969
2006	150	9.06	1359	5.837	0.052912
2007	82	6.01	492	3.191	0.019169
2008	128	8.93	1142	4.982	0.044465
2009	140	7.99	1118	5.448	0.043546
2010	85	5.91	502	3.306	0.019542
2011	64	5.01	320	2.49	0.012463
2013	15	5.64	84	0.584	0.003291
2014	13	7.06	91	0.506	0.003569
2015	23	5.73	131	0.895	0.005128
2016	22	5.59	122	0.856	0.004787
2017	18	5.73	103	0.7	0.004013
2018	146	4.89	713	5.682	0.02779
2019	62	4.06	251	2.412	0.009793
2020	98	4.23	414	3.813	0.016121
2021	70	5.24	366	2.723	0.014281
2022	145	6.10	884	5.643	0.034419
2023	191	6.92	1321	7.432	0.051426
2024	151	6.03	910	5.876	0.035444

Table S17: Annual count, annual mean area (ha), annual sum of area (ha), annual count density (d = count/100 ha), and annual sum of area density (d = sum of area ha/100 ha) results for mining within Key Biodiversity Areas in

Guyana. *Note: 2012 is omitted due to the transition between Landsat 5 TM and Landsat 8 OLI. Landsat 7 ETM+ was excluded because of SLC-off artefacts, resulting in insufficient consistent imagery for that year. Additionaly, 2002 and 2010 are ommited due to no data available.*

Year	Count	Mean Area (ha)	Sum of Area (ha)	Count (d)	Sum of Area (d)
1995	2	25.41	50	3.241	0.082404
1996	16	9.8	156	25.928	0.254161
1997	2	5.84	11	3.241	0.018929
1998	2	6.2	12	3.241	0.02011
1999	8	13.6	108	12.965	0.176334
2000	5	3.93	19	8.103	0.031865
2001	8	6.31	50	12.965	0.081843
2002	No Data	No Data	No Data	No Data	No Data
2003	7	5.08	35	11.349	0.057605
2004	12	8.21	98	19.448	0.159688
2005	20	10.92	218	32.411	0.354108
2006	14	10.8	151	22.689	0.244949
2007	5	5.16	25	8.103	0.041863
2008	28	9.74	272	45.39	0.442087
2009	9	4.19	37	14.593	0.061143
2010	No Data	No Data	No Data	No Data	No Data
2011	5	8.6	42	8.103	0.069672
2013	6	3.61	21	9.729	0.03509
2014	4	6.82	27	6.486	0.044218
2015	9	25.02	225	14.593	0.365009
2016	7	7.37	51	11.349	0.083639
2017	16	15.18	242	25.928	0.393865
2018	10	11.85	118	16.209	0.19203
2019	4	3.06	12	6.486	0.019814
2020	6	10.29	61	9.729	0.100089
2021	10	9.05	90	16.209	0.146649
2022	36	16.51	594	58.335	0.963833
2023	36	10.95	394	58.335	0.639245
2024	26	17.97	467	42.126	0.757239

Table S18: Annual count, annual mean area (ha), annual sum of area (ha), annual count density (d = count/100 ha), and annual sum of area density (d = sum of area ha/100 ha) results for mining within Key Biodiversity Areas in Suriname. *Note: 2012 is omitted due to the transition between Landsat 5 TM and Landsat 8 OLI. Landsat 7 ETM+ was excluded because of SLC-off artefacts, resulting in insufficient consistent imagery for that year.*

Year	Count	Mean Area (ha)	Sum of Area (ha)	Count (d)	Sum of Area (d)
1995	3	3.86	11	0.064	0.000247
1996	6	3.75	22	0.128	0.00048
1997	8	5.54	44	0.171	0.000946

1998	8	6.10	48	0.171	0.001042
1999	10	7.44	74	0.213	0.001587
2000	14	6.06	84	0.299	0.001812
2001	20	6.90	138	0.427	0.002945
2002	10	7.88	78	0.213	0.001682
2003	38	9.55	362	0.811	0.007746
2004	45	12.99	584	0.96	0.012469
2005	52	15.22	791	1.11	0.016894
2006	67	15.33	1027	1.43	0.021911
2007	43	15.64	672	0.917	0.014348
2008	77	12.69	976	1.643	0.020851
2009	76	14.92	1133	1.621	0.024203
2010	55	12.70	698	1.174	0.014907
2011	94	14.71	1382	2.007	0.029509
2013	118	23.86	2815	2.518	0.060098
2014	117	33.76	3950	2.497	0.084345
2015	128	36.72	4699	2.731	0.100398
2016	128	41.72	5340	2.731	0.113936
2017	142	38.47	5463	3.031	0.116622
2018	130	42.78	5560	2.774	0.11867
2019	162	33.86	5485	3.456	0.117048
2020	161	36.26	5837	3.436	0.124578
2021	150	34.69	5203	3.2	0.111062
2022	148	43.00	6363	3.157	0.135843
2023	161	44.10	7099	3.436	0.151512
2024	135	40.71	5495	2.881	0.117289

Table S19: Annual count, annual mean area (ha), annual sum of area (ha), annual count density (d = count/100 ha), and annual sum of area density (d = sum of area ha/100 ha) results for mining outside of protected areas, Key Biodiversity Areas, and Indigenous lands across the combined Guyanas. *Note: 2012 is omitted due to the transition between Landsat 5 TM and Landsat 8 OLI. Landsat 7 ETM+ was excluded because of SLC-off artefacts, resulting in insufficient consistent imagery for that year.*

Year	Count	Mean Area (ha)	Sum of Area (ha)	Count (d)	Sum of Area (d)
1995	465	14.12	6565	2.75	0.04
1996	756	10.70	8087	4.47	0.05
1997	995	13.02	12950	5.88	0.08
1998	976	13.73	13395	5.77	0.08
1999	945	12.87	12157	5.59	0.07
2000	1131	14.21	16072	6.69	0.10
2001	1124	14.84	16679	6.65	0.10
2002	240	10.54	2530	1.42	0.02
2003	1807	16.53	29861	10.69	0.18
2004	2299	16.29	37445	13.60	0.22
2005	2456	16.38	40221	14.53	0.24

2006	2836	15.60	44247	16.77	0.26
2007	1425	13.31	18959	8.43	0.11
2008	3039	17.87	54317	17.97	0.32
2009	2838	16.75	47530	16.79	0.28
2010	2100	12.40	26048	12.42	0.15
2011	2609	15.00	39131	15.43	0.23
2013	4857	17.33	84181	28.72	0.50
2014	4886	19.57	95601	28.89	0.57
2015	5779	19.39	112074	34.18	0.66
2016	5792	20.10	116413	34.26	0.69
2017	6285	21.11	132666	37.17	0.78
2018	5622	20.23	113714	33.26	0.67
2019	5589	20.25	113179	33.05	0.67
2020	6526	21.95	143244	38.62	0.85
2021	5742	21.32	122416	33.96	0.72
2022	7225	22.79	164621	42.72	0.97
2023	8079	26.48	213927	47.78	1.27
2024	6951	20.52	142598	41.12	0.84

Table S20: Annual count, annual mean area (ha), annual sum of area (ha), annual count density (d = count/100 ha), and annual sum of area density (d = sum of area ha/100 ha) results for mining outside of protected areas, Key Biodiversity Areas, and Indigenous lands within French Guiana. *Note: 2012 is omitted due to the transition between Landsat 5 TM and Landsat 8 OLI. Landsat 7 ETM+ was excluded because of SLC-off artefacts, resulting in insufficient consistent imagery for that year.*

Year	Count	Mean Area (ha)	Sum of Area (ha)	Count (d)	Sum of Area (d)
1995	90	14.68	1321	26.98	0.40
1996	154	13.13	2022	46.19	0.61
1997	262	17.00	4453	78.60	1.34
1998	255	13.52	3447	76.51	1.03
1999	291	15.31	4454	87.28	1.34
2000	390	16.06	6261	116.92	1.88
2001	361	14.31	5164	108.31	1.55
2002	32	11.95	382	9.59	0.12
2003	672	17.02	11435	201.58	3.43
2004	688	17.12	11779	206.33	3.53
2005	669	15.50	10369	200.73	3.11
2006	802	16.24	13026	240.64	3.91
2007	507	12.34	6254	152.08	1.88
2008	740	16.78	12417	221.91	3.73
2009	782	15.94	12463	234.54	3.74
2010	476	11.18	5323	142.73	1.60
2011	497	11.26	5597	149.02	1.68
2013	483	11.74	5672	144.81	1.70

2014	622	15.10	9394	186.51	2.82
2015	595	13.48	8023	178.44	2.41
2016	650	12.29	7985	194.96	2.40
2017	644	14.04	9041	193.19	2.71
2018	657	11.72	7702	197.00	2.31
2019	590	10.94	6456	176.86	1.94
2020	785	12.36	9700	235.35	2.91
2021	560	11.96	6698	167.98	2.01
2022	1022	12.43	12701	306.57	3.81
2023	1108	14.49	16057	332.38	4.82
2024	715	11.09	7927	214.39	2.38

Table S21: Annual count, annual mean area (ha), annual sum of area (ha), annual count density (d = count/100 ha), and annual sum of area density (d = sum of area ha/100 ha) results for mining outside of protected areas, Key Biodiversity Areas, and Indigenous lands within Suriname. *Note: 2012 is omitted due to the transition between Landsat 5 TM and Landsat 8 OLI. Landsat 7 ETM+ was excluded because of SLC-off artefacts, resulting in insufficient consistent imagery for that year.*

Year	Count	Mean Area (ha)	Sum of Area (ha)	Count (d)	Sum of Area (d)
1995	87	11.15	970	0.20	0.02
1996	188	12.34	2319	0.44	0.05
1997	323	14.36	4636	0.75	0.11
1998	389	13.16	5120	0.90	0.12
1999	413	13.90	5738	0.96	0.13
2000	438	15.22	6664	1.02	0.16
2001	462	19.08	8816	1.07	0.20
2002	177	10.83	1916	0.41	0.04
2003	617	19.61	12096	1.43	0.28
2004	804	19.59	15747	1.86	0.37
2005	810	18.02	14599	1.88	0.34
2006	900	17.50	15752	2.09	0.37
2007	729	14.65	10676	1.69	0.25
2008	951	19.93	18949	2.20	0.44
2009	1107	19.49	21575	2.57	0.50
2010	888	13.70	12163	2.06	0.28
2011	959	17.16	16456	2.22	0.38
2013	1360	19.98	27169	3.15	0.63
2014	1396	26.88	37523	3.24	0.87
2015	1504	27.23	40959	3.49	0.95
2016	1513	29.60	44777	3.51	1.04
2017	1512	27.51	41589	3.50	0.96
2018	1568	27.02	42372	3.63	0.98
2019	1675	28.36	47495	3.88	1.10
2020	1750	29.21	51109	4.06	1.19

2021	1591	27.54	43814	3.69	1.02
2022	1842	32.25	59412	4.27	1.38
2023	1943	36.15	70228	4.50	1.63
2024	1863	25.94	48324	4.32	1.12

Table S22: Annual count, annual mean area (ha), annual sum of area (ha), annual count density (d = count/100 ha), and annual sum of area density (d = sum of area ha/100 ha) results for mining outside of protected areas, Key Biodiversity Areas, and Indigenous lands within Guyana. *Note: 2012 is omitted due to the transition between Landsat 5 TM and Landsat 8 OLI. Landsat 7 ETM+ was excluded because of SLC-off artefacts, resulting in insufficient consistent imagery for that year.*

Year	Count	Mean Area (ha)	Sum of Area (ha)	Count (d)	Sum of Area (d)
1995	288	14.84	4274	2.35	0.035
1996	414	9.05	3746	3.38	0.031
1997	410	9.42	3860	3.35	0.032
1998	332	14.54	4827	2.71	0.039
1999	241	8.15	1964	1.97	0.016
2000	303	10.38	3145	2.47	0.026
2001	301	8.96	2697	2.46	0.022
2002	31	7.47	231	0.25	0.002
2003	518	12.22	6329	4.22	0.052
2004	807	12.29	9917	6.58	0.081
2005	977	15.61	15252	7.97	0.124
2006	1134	13.64	15468	9.25	0.126
2007	189	10.73	2028	1.54	0.017
2008	1348	17.03	22949	10.99	0.187
2009	949	14.22	13491	7.74	0.110
2010	736	11.63	8561	6.00	0.070
2011	1153	14.81	17077	9.40	0.139
2013	3014	17.03	51340	24.59	0.419
2014	2868	16.98	48683	23.38	0.397
2015	3680	17.15	63091	30.01	0.515
2016	3629	17.54	63650	29.60	0.519
2017	4129	19.87	82035	33.67	0.669
2018	3397	18.73	63639	27.71	0.519
2019	3324	17.82	59226	27.11	0.483
2020	3991	20.66	82434	32.57	0.672
2021	3591	20.02	71903	29.31	0.587
2022	4361	21.21	92508	35.59	0.754
2023	5028	25.39	127641	41.00	1.041
2024	4373	19.75	86346	35.67	0.704